

## Seasonality of aerosol chemical composition at King Sejong Station (Antarctic Peninsula) in 2013

Sang-bum Hong<sup>a,\*</sup>, Young Jun Yoon<sup>a</sup>, Silvia Becagli<sup>b,\*\*</sup>, Yeontae Gim<sup>a</sup>, S.D. Chambers<sup>c</sup>, Ki-Tae Park<sup>a</sup>, Sang-Jong Park<sup>a</sup>, Rita Traversi<sup>b</sup>, Mirko Severi<sup>b</sup>, V. Vitale<sup>d</sup>, Joo-Hong Kim<sup>a</sup>, Eunho Jang<sup>a,e</sup>, J. Crawford<sup>c</sup>, A.D. Griffiths<sup>c</sup>

<sup>a</sup> Korea Polar Research Institute (KOPRI), 26 Songdomirae-ro, Yeosu-gu, Incheon, 21990, South Korea

<sup>b</sup> Department of Chemistry "Ugo Schiff" – University of Florence, Florence, Italy

<sup>c</sup> ANSTO, Environmental Research, Locked Bag 2001, Kirrawee DC NSW, 2232, Australia

<sup>d</sup> ISAC-CNR, Bologna, Italy

<sup>e</sup> University of Science and Technology, 217 Gajeong-ro, Yuseong-gu, Daejeon, 34113, South Korea

### ARTICLE INFO

#### Keywords:

PM<sub>10</sub> and PM<sub>2.5</sub> aerosol  
King sejong station  
Seasonal variations of ionic components  
Sea spray  
Biogenic sulphur compounds  
Ammonium

### ABSTRACT

Seasonal variations of ionic species concentrations in PM<sub>10</sub> and PM<sub>2.5</sub> aerosols were investigated at King Sejong Station (King George Island, Antarctic Peninsula) in 2013. Seasonal variations of PM<sub>2.5</sub> mass were also determined, and found to be in the range: 2482.2 ± 944.4 ng m<sup>-3</sup> (austral winter) to 3493.3 ± 1223.8 ng m<sup>-3</sup> (austral fall). On a weight basis, the PM<sub>2.5</sub> ionic species consisted mainly of primary ions from sea spray (~30% in summer, ~50% in winter) and partly from secondary ions (~20% in summer), with the ratios of sea spray and secondary ion components to PM<sub>2.5</sub> mass showing clear seasonal variation. The seasonal cycle of sea spray components was not well defined, but was weakly correlated with wind speed ( $r^2 = 0.38$ ). This correlation was likely attributable to a combination of the seasonal properties of wind and the measurement site's location at the western tip of Barton Peninsula. The concentrations of sulphur species (CH<sub>3</sub>SO<sub>3</sub><sup>-</sup> and non sea salt SO<sub>4</sub><sup>2-</sup>) were clearly higher during austral summer. Notably, these concentrations were ~2–3 times higher during in January 2013 than in other summer months of the field observation period. This was attributed to an increased biomass of algae in the ocean area surrounding King George Island and more frequent air mass passage over ocean areas with algae blooms. The NH<sub>4</sub><sup>+</sup> concentration was also clearly higher in austral summer 2013, mainly due to secondary formation from the NH<sub>3</sub> released from local emission sources such as penguin colonies and ocean areas near the measurement site with acidic aerosol, but also affected by local meteorology specific to the summer of 2014.

### 1. Introduction

Antarctica is a remote and typically isolated region, due in part to the strong westerly flows in the atmosphere and Southern Ocean that surround it. It is therefore considered to be the most suitable location to investigate the physico-chemical properties of a primitive version of earth's atmosphere. Antarctica is very important in regulating global oceanic and atmospheric circulation and responsive to even small changes in global surface and ocean temperatures. In particular, the Antarctic Peninsula region has experienced rapid environmental changes over the past several decades such as diminishing of the

Antarctic ice sheets and a warming of several K (Vaughan and Doake, 1996; Vaughan et al., 2003). This is believed to have been driven primarily by increasing westerly winds associated with the formation of the ozone hole in the lower stratosphere over Antarctica (Thompson and Solomon, 2002; Marshall, 2003). These changes indicate just how sensitive the Antarctic Peninsula and its atmospheric environment are to global warming of the last century, which has resulted from changes in global atmospheric composition. Consequently, the Antarctic Peninsula is a key region for monitoring the effects of global warming on Antarctica, so consistent monitoring of the properties of climate related atmospheric components (gases and aerosols) in this region is crucial.

\* Corresponding author.

\*\* Corresponding author.

E-mail addresses: [hong909@kopri.re.kr](mailto:hong909@kopri.re.kr) (S.-b. Hong), [silvia.becagli@unifi.it](mailto:silvia.becagli@unifi.it) (S. Becagli).

<https://doi.org/10.1016/j.atmosenv.2019.117185>

Received 17 June 2019; Received in revised form 6 November 2019; Accepted 25 November 2019

Available online 26 November 2019

1352-2310/© 2019 Elsevier Ltd. All rights reserved.

It has been well established that aerosols directly and indirectly play an important role in regional and global climate because their chemical and physical properties can alter atmospheric radiative properties (Shaw, 1988; Tang, 1996). A thorough analysis of aerosols is therefore necessary for any investigation of regional climatic effects. However, since mean aerosol characteristics can change markedly with disproportionately small changes in measurement location or sampling time, it is not trivial to make representative aerosol observations at the regional scale. It is therefore necessary to make consistent measurements over multiple years to reduce uncertainties in their climatic influences at key sites (Weller et al., 2011).

Systematic aerosol research programs have been conducted at a number of coastal and inland Antarctic research stations since the middle of 1990s to improve understanding of their chemical properties (Wolff et al., 1998). However, with the exception of a few multi-year aerosol programs at coastal (65–70°S) and inland Antarctic stations (e.g. Halley: Wolff et al., 1998; Neumayer: Weller et al., 2011; Dumont D'Urville: Legrand et al., 2017a, 2017b; Dome Concordia: Traversi et al., 2014; Zhongshan: Zhang et al., 2015; and South Pole: Sheridan et al., 2016), most experiments have been performed only during austral summer conditions due to the difficulties of maintaining aerosol samplers in the field. The multi-year observations have been used to identify seasonal and inter-annual variations of aerosol component concentrations, hypothesize emission sources, and investigate transport pathways from source areas to measurement sites. Some of these studies have reported aerosol transport to Antarctica from continental regions in low to middle latitudes of the Southern Hemisphere (Legrand et al., 1998; Li et al., 2008), or input from stratosphere (Wagenbach et al., 1998; Savarino et al., 2007; Traversi et al., 2017).

However, few results have been published from the sub-Antarctic region (60–65°S) between mid-Southern Hemisphere latitudes and Antarctica (Artaxo et al., 1992; Savoie et al., 1993; Mishra et al., 2004; Asmi et al., 2018; Lim et al., 2019). King Sejong Station (Global Atmosphere Watch code "KSG") is located near the northern tip of the Antarctic Peninsula at 62°S, on Barton Peninsula of King George Island (KGI). It is therefore an important site from which to investigate characteristics of the Southern Ocean atmosphere in the sub-Antarctic.

Regarding the existing KGI aerosol studies, Artaxo et al. (1992) was first to report mass concentrations of fine ( $d_p < 2.0 \mu\text{m}$ ) and coarse ( $2.0 \mu\text{m} < d_p < 15 \mu\text{m}$ ) particles, and the seasonal cycle of non-sea salt (nss) sulphur (element) with a winter minimum at Ferraz station (KGI) based on observations between 1985 and 1988. Mishra et al. (2004) reported temporal variability of major metals and ions in TSP at KSG, as well as the associated source processes, for measurements from 2001 to 2002. They found that most metals and ions exhibited maximum values in spring and summer, and that both natural and anthropogenic source processes can influence the chemical composition of TSP due to the unique geographical location and meteorological conditions of KSG. Recently, Lim et al. (2019) also investigated the chemical characteristics of submicron aerosols ( $\text{PM}_{10}$ ) observed at KSG. They found that organic matter and sea salts comprised 85% of the  $\text{PM}_{10}$  and organic carbon concentration was the highest in fall. The physical properties of aerosol particles at KSG have been monitored since March 2009.

Recently, Kim et al. (2017) reported a clear seasonal variation in particle number concentration (CN) with a maximum in austral summer (December, January and February) and minimum in austral winter (June, July and August) based on in-situ measured aerosol data between March 2009 and February 2015. In 2013 an aerosol chemistry monitoring program was run year-round at KSG by the Korea Polar Research Institute (KOPRI), in collaboration with the University of Florence (UOF; Italy). The primary aim of this program was to provide further insights into the chemical properties of  $\text{PM}_{10}$  and  $\text{PM}_{2.5}$  aerosols in the atmosphere around KGI. It is therefore expected that the results of this study will further clarify and build upon the results of Mishra et al. (2004) and Lim et al. (2019), who reported several important aspects of aerosol chemistry in this region.

The objective of this study is to characterize the seasonality of mass and ionic species concentrations (primary sea salt aerosol,  $\text{NH}_4^+$ , non-sea salt (nss)  $\text{SO}_4^{2-}$ , and  $\text{CH}_3\text{SO}_3^-$ ) in aerosols whose aerodynamic size are less than  $10 \mu\text{m}$  ( $\text{PM}_{10}$ ;  $d_{50} < 10 \mu\text{m}$ ), collected using integrated filter-based aerosol sampling with a time resolution from one day to 1 week at KSG in 2013, and the major processes responsible for them. Even though the temporal resolution of filter-based measurements of this study is insufficient to observe variations in aerosol chemical properties occurring on sub-diurnal timescales, they have generally been made to determine the seasonality of Antarctic aerosol components because of the comparatively very low aerosol loading in Antarctic regions.

Until now, there have been no scientific reports about these issues in  $\text{PM}_{2.5}$  and  $\text{PM}_{10}$  collected at the same time at KGI. This article also reports seasonal variations of  $\text{PM}_{2.5}$  mass and ionic compositions with respect to  $\text{PM}_{2.5}$  mass for year round observations at KGI for the first time. The seasonalities of sea spray, biogenic sulphur and ammonium species are investigated in detail with respect to changes of source intensity, transport efficiency to the measurement site, meteorology and atmospheric chemistry between basic gas and acidic aerosol. Based on these, major factors affecting seasonalities of these species are specifically identified and, especially, the importance of ammonia gas to influence temporal variations of  $\text{NH}_4^+$  in aerosols are also suggested. It should be noted that Mishra et al. (2004) did not suggest the major factors responsible for the seasonal variations of ionic species in TSP, despite seasonal aerosol characteristics and information about their main drivers being essential for a complete understanding of Antarctic climate variability.

## 2. Methods

### 2.1. Measurement site and meteorology

KSG (62°13'S, 58°47'W; ~10 m a.s.l.) is a coastal sub-Antarctic site located on the western tip of Barton Peninsula on KGI, South Shetland Islands (Fig. S1). KGI is widely recognised as a comparatively densely populated region of Antarctica due to a large number of multinational field research activities that are conducted during the summer seasons and station operations by overwintering crews (Mishra et al., 2004; Pereira et al., 2006; Shirsat and Graf, 2009). Five of the six nearby Antarctic stations are ~7–10 km northwest of KSG, across Maxwell Bay, and one is located ~7 km southeast of KSG beyond a mountain glacier. KGI has been the focal point of numerous biological research programs, and the region contains 7 Antarctic Special Protection Areas (ASPAs). Of these, ASPA 171 (Narebski Point Penguin Colony) is ~2 km southeast of KSG on Barton Peninsula (Fig. S2).

Meteorological parameters at KSG were measured using an automatic meteorological observation system (AMOS), for which the exact location and sensor specifications have been described by Choi et al. (2008), Chambers et al. (2014) and Kim et al. (2017). Briefly, over 2013 temperatures ranged between  $-20.3$  and  $7.7$  °C, with a mean of  $-2.2$  °C. The mean wind speed, relative humidity, and cloud amount were  $8.2 \text{ m s}^{-1}$ , 89.2%, and 6.8 octas, respectively. Wind directions were NW throughout most of the year, with the frequency of easterly winds increasing in winter. Due to its geographic location near the Polar Front, KSG experiences the frequent passage of mesoscale or synoptic depressions, which results in frequent precipitation or cloudy days (Choi et al., 2008).

### 2.2. Aerosol measurements

The field observation period (FOP) for this study was from 14 January 2013 to 18 January 2014. The operation of all aerosol samplers was based on universal time control (UTC) (KSG local standard time = UTC-4hrs) and the Southern Hemisphere seasonal convention has been adopted. It should be noted that atmospheric components at Global

Atmosphere Watch baseline or background sites such as KSG, should be collected only in designated “clean air sectors” due to the high directional sensitivity to anthropogenic activity and typically low ambient concentrations. Because the KSG atmospheric observation building (AOB) was 200–300m SW of the main station buildings and incinerator, air pumps of all PM samplers were controlled to automatically shut down for wind speeds less than  $1.0 \text{ m s}^{-1}$ , or when wind direction entered the sector  $350\text{--}70^\circ$ , which has been identified as being responsible for most anthropogenic pollution signals in atmospheric measurements at this site (Kim et al., 2017). Considering the color of Quartz filters (sampling time:  $\sim 2$  weeks) during FOP, showing no visible observation of grayness, the effect of local contamination from KSG station activities was very weak due to the deployment of the wind sector controller.

Three approaches were used to determine the chemical characteristics of ionic species in KSG aerosols as follows (Fig. S3a):  $\text{PM}_{10}$  bulk sampling (sample collection period: 1 day);  $\text{PM}_{10}$  size segregating sampling (sample collection period: 3 days); and  $\text{PM}_{2.5}$  ( $d_{50} < 2.5 \mu\text{m}$ ) bulk sampling combined with two denuder tubes (sample collection period: 7 days). This study focuses only on the masses and ionic species in aerosols collected using the  $\text{PM}_{10}$  and  $\text{PM}_{2.5}$  bulk samplers.

The duration of individual aerosol sample collections from these samplers was varied according to the total air volume passing through the filters, because it's difficult to operate them normally under harsh meteorological conditions (like blizzards) and wind directions in the sector  $350\text{--}70^\circ$ .

#### 2.2.1. $\text{PM}_{2.5}$ collector combined with denuder tubes (KOPRI)

$\text{PM}_{2.5}$  aerosols were collected on a Teflon filter (Zefluor 47 mm  $\phi$ , 2.0  $\mu\text{m}$  pore size, Gelman Sciences, USA) installed in the first of three-stages of the filter assembly. These aerosols go through both the  $\text{PM}_{2.5}$  cut off impactor (TCR impactor, TCR, ITALY) and two annular coated denuders (URG-2000-30, 242 mm, 3CSS, URG, USA) in series installed to remove acidic and basic gases at a flow rate of  $38.3 \text{ L min}^{-1}$ . Quartz (Tissuquartz 47 mm  $\phi$ , Pall, USA) and Nylon (Nylarsorb 47 mm  $\phi$ , 1.0  $\mu\text{m}$  pore size, Pall, USA) filters were also installed in the second and third stages, respectively, to capture gaseous species that might otherwise be evaporated from semi-volatile species such as  $\text{NH}_4\text{NO}_3$  and  $\text{NH}_4\text{Cl}$  in  $\text{PM}_{2.5}$  collected on the Teflon filter over the sample collection period (Table S1 and Fig. S3b).

Teflon filters were installed with no pre-cleaning step for drying in order to weigh their masses, but Quartz and Nylon filters were first soaked in a pre-cleaned glass dish filled with ultra pure water (UPW) from a Mill-Q system (Millipore, USA) for  $\sim 2$  days in order to decrease the blank levels of the filter itself. They were prepared on a class 10 clean bench (ISO 4) of a class 1000 clean room (ISO 6). After rinsing with UPW, filters were dried and capped in a pre-cleaned Petri dish. The Quartz filters were then first immersed in a 1% Citric acid (ACS grade)/25% Glycerol (ACS grade) solution and then dried on a class 10 clean bench (ISO 4).

Despite these precautions, based on a comparison of concentrations of concerned ions ( $\text{NH}_4^+$ ,  $\text{Cl}^-$  and  $\text{NO}_3^-$ ) (Fig. S4), variability in  $\text{NH}_4^+$  concentration could be quite sensitive to the quartz filter blank levels because they were not controlled to be low enough in the cleaning step.  $\text{Cl}^-$  and  $\text{NO}_3^-$  results from the Nylon filter behind the Quartz filter implied a very weak conversion to the gaseous phase during sampling periods because they are very similar with those of blank values, showing they are almost within the range of the standard deviation of mean values of the blank filters. Consequently, the concentrations of  $\text{PM}_{2.5}$  ionic species in this study indicate their levels only in the particle phase, not the sum from both particle phase and gas phase captured after evaporation.

The two denuders were coated according to the procedure described by Hong et al. (2009). The inner surface of the denuders was coated with  $\sim 10 \text{ mL}$  of fresh coating solution and then totally dried by nitrogen ( $\text{N}_2$ ) gas (1 bar, 5 SLPM, purity  $> 99.999\%$ ) for  $\sim 30 \text{ min}$  in the KSG AOB

during the FOP. The temperature inside the denuder box was set at  $\sim 5^\circ\text{C}$ .

Air flow rate was controlled using a custom built orifice, calibrated in a laboratory with a mass flow controller using the same vacuum pump deployed at KSG for the  $\text{PM}_{2.5}$  aerosol sampler. A dry gas meter (DC-5, SHINAGAWA, JAPAN) was installed before the air pump to measure total air flow rates during each sampling period.  $\text{PM}_{2.5}$  sampling periods were varied to ensure sampling of over  $300 \text{ m}^3$ , a value determined considering the typical ambient  $\text{PM}_{2.5}$  mass and detection limits of ionic species using the ion chromatography system.

Teflon filters were weighed before and after aerosol collections with an electric balance (XP-205, Mettler Toledo, SWISS) of 0.01 mg readability installed at Jeju National University (JNU). According to Song et al. (2017), they were dried in desiccator (DU.2478169, Duran®, Germany) filled with silicagel blue (CP, D.J, KOREA) in the laboratory. Teflon filters were then weighed every day for  $\sim 7$  days, and their masses finally recorded when masses measured on successive days were almost the same. After determining each filter's mass, they were kept in a pre-cleaned Petri dish with UPW until use.

#### 2.2.2. $\text{PM}_{10}$ sampler (UOF)

Operation of the UOF  $\text{PM}_{10}$  sampler and preparation of the filters followed the procedure described by Udisti et al. (2012). In this study, the 24-h integrated filter-based  $\text{PM}_{10}$  samples were generally collected between  $\sim 20:00 \text{ p.m. (UTC 00:00)}$  and  $\sim 20:00 \text{ p.m.}$

#### 2.3. $^{222}\text{Rn}$ gas measurement

Hourly measurements of atmospheric radon concentrations have been made at KSG since February 2013 using a 1500 L dual-flow-loop two-filter radon detector manufactured by ANSTO. This is a direct (not “by-progeny”) measurement system that specifically targets the isotope  $^{222}\text{Rn}$  ( $t_{1/2} = 3.82 \text{ days}$ ). The setup, calibration and operation of this detector throughout the FOP of this study has already been described in detail by Chambers et al. (2014). Further information regarding the sensitivity and detection limits of dual-flow-loop two-filter radon detectors operating in Antarctica can be found in Chambers et al. (2018).

#### 2.4. Ion extraction and analysis

The extraction methods and analysis techniques for deriving ionic species in the KOPRI  $\text{PM}_{2.5}$  samples are described in detail below. In the case of the UOF  $\text{PM}_{10}$  samples, extraction and analysis were performed according to the methods of Udisti et al. (2012).

##### 2.4.1. $\text{PM}_{2.5}$ processing

After sampling, gaseous species collected in the coated annular denuders were extracted in the KSG AOB by shaking denuder tubes for  $\sim 5\text{--}10 \text{ min}$  in 30 mL ultra-pure water (UPW). We investigated extraction efficiencies of ionic species from denuder tubes after extracting them with 30 mL UPW repeatedly and the extraction efficiencies of  $\text{Cl}^-$ ,  $\text{NO}_3^-$ ,  $\text{SO}_4^{2-}$  and  $\text{NH}_4^+$  were over  $\sim 95\%$ .

Extraction solutions from the denuders and all filters were refrigerated at about  $-20^\circ\text{C}$  in the KSG research building during the FOP. All filters were handled inside a class 10 clean bench (ISO 4) of a class 1000 clean room (ISO 6) of KOPRI. To extract ionic species from the Teflon filters, each filter was put into an extraction vial (WH.986701, Wheaton, UAS), and wet with 0.2 mL of HPLC grade ethanol to enhance the hydrophilicity of the Teflon filter surface. Filters were then extracted in an ultrasonic bath (Power sonic 520, Korea) for 30 min with 20 mL UPW, and were then mechanically shaken (SH-502, Seyoung, Korea) for 60 min. All extracts were filtered by syringe filters (Ion chromatography Acrodisc 13 mm  $\phi$ , 0.45  $\mu\text{m}$  pore size, Pall life science, USA). The Quartz and Nylon filters were also put into an extraction vial, but then just extracted in the ultrasonic bath for 30 min with 20 mL DW. Extracts

from the Quartz filters were also filtered with the same kind of syringe filter used for the Teflon filters. However, extracts from Nylon filters were simply stored in the refrigerator with no filtration process.

Ionic species from all extracts were analyzed within a week of preparation using an ion chromatography (IC) system. An analysis column of ionic species, IonPac CS12A ( $4 \times 250$  mm, thermo, USA) was used for cations, and IonPac AS15 ( $2 \times 250$  mm, thermo, USA) was used for anions. The analysis conditions, including eluent concentration, instrument detection limits (IDLs), and coefficients of variation (CVs) according to concentration levels were described in detail by Hong et al. (2015). The accuracy test for cations and anions was typically 5%, except for  $\text{NH}_4^+$  which was  $\sim 10\%$ . The anions, especially  $\text{NO}_3^-$ , in samples extracted from denuder tubes coated with  $\text{Na}_2\text{CO}_3$ , were compared with data analyzed using the carbonate eluent IC system for their certification. Analytical conditions for the analysis of anions in the carbonate eluent IC system have been described by Song et al. (2016). Because  $\text{CO}_3^{2-}$  could be dissolved from the  $\text{Na}_2\text{CO}_3$  coating on the inner surface of denuder during the preparation step,  $\text{CO}_3^{2-}$  peak area of the IC system using the potassium hydroxide (KOH) eluent greatly increased. However,  $\text{NO}_3^-$  was rarely influenced by this interference.

Filter blanks from KOPRI  $\text{PM}_{2.5}$  Teflon filters were extracted to certify the cleanness of filters and summarized in Table S2. Blank levels of ions from UOF daily  $\text{PM}_{10}$  sampler were usually below the detection limit or least one order of magnitude lower than 10 percentile of sample data.

## 2.5. Back trajectories and cluster analysis

3-day air mass back trajectories were calculated using the PC version of HYSPLIT v4.0 [Hybrid Single-Particle Lagrangian Integrated Trajectory; Draxler and Rolph, 2003]. The arrival height was 500 m above ground level, since this elevation is normally representative of atmospheric mixing height at KSG during summer. These calculations were based on meteorological data of  $1^\circ \times 1^\circ$  resolution generated by the global data assimilation system (GDAS) model run by the National Weather Service's (NWS) National Centre for Environmental Prediction (NCEP). In view of the increasing uncertainty of the hind-casts back in time (e.g. Stohl, 1998), since the fetch regions we were primarily interested in observing were within the typical 3-day fetch region, we limited the extent of trajectories used to form our clusters to 3-days to try to make them more representative of surrounding fetch regions. Cluster analyses were also performed based on 3-day air mass back trajectories at 00 UTC each day. Details regarding the clustering algorithm are provided on the ARL NOAA site ready.arl.noaa.gov/HYSPLIT.php.

## 3. Results

### 3.1. General overview

Figs. 1–3 show concentration variations of ionic components in  $\text{PM}_{2.5}$  and  $\text{PM}_{10}$  during the FOP. Because  $\text{PM}_{2.5}$  samples were collected after passing denuder tubes to capture gaseous species, concentrations of

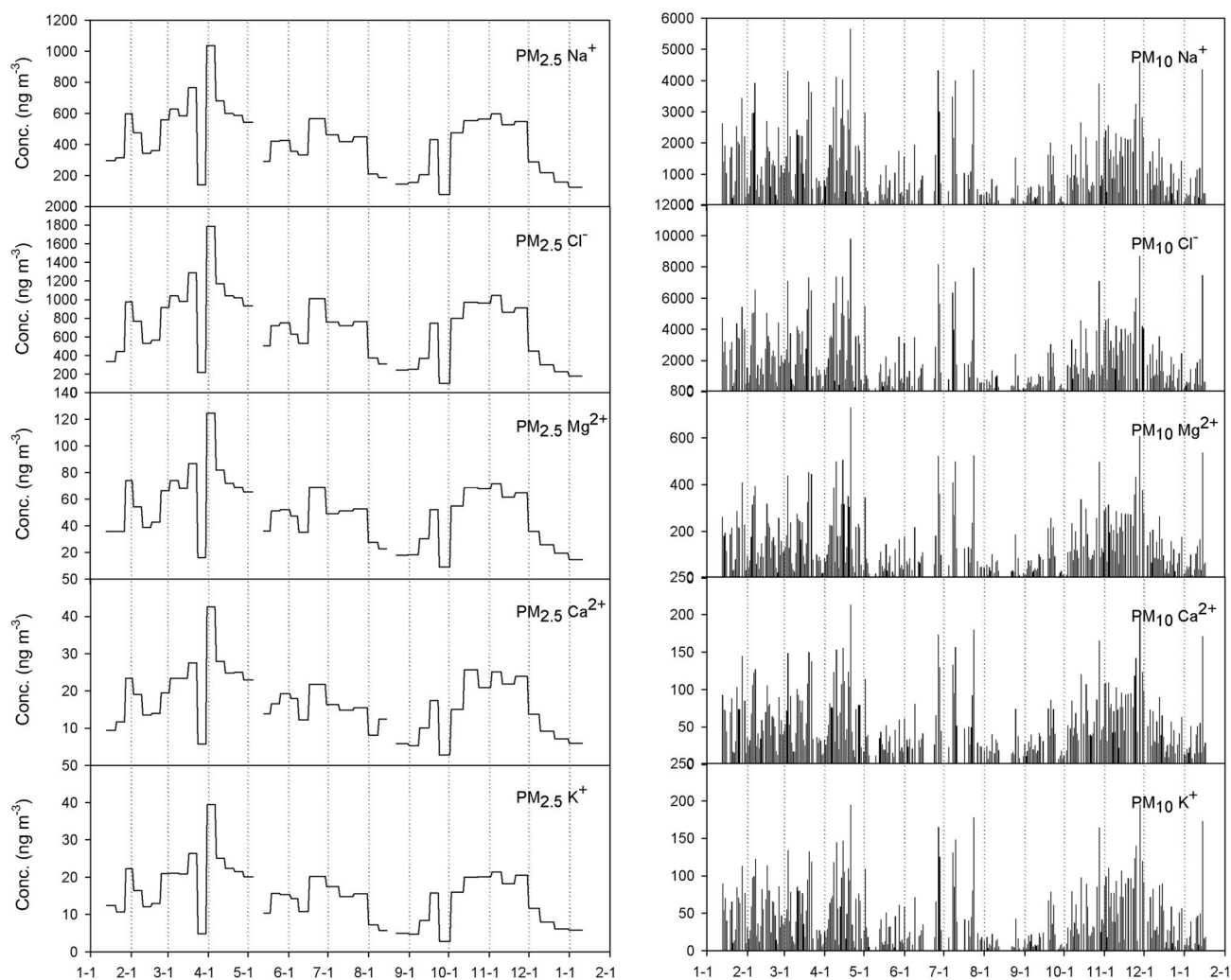


Fig. 1. Concentration variations of components from sea spray from  $\text{PM}_{2.5}$  and  $\text{PM}_{10}$ .

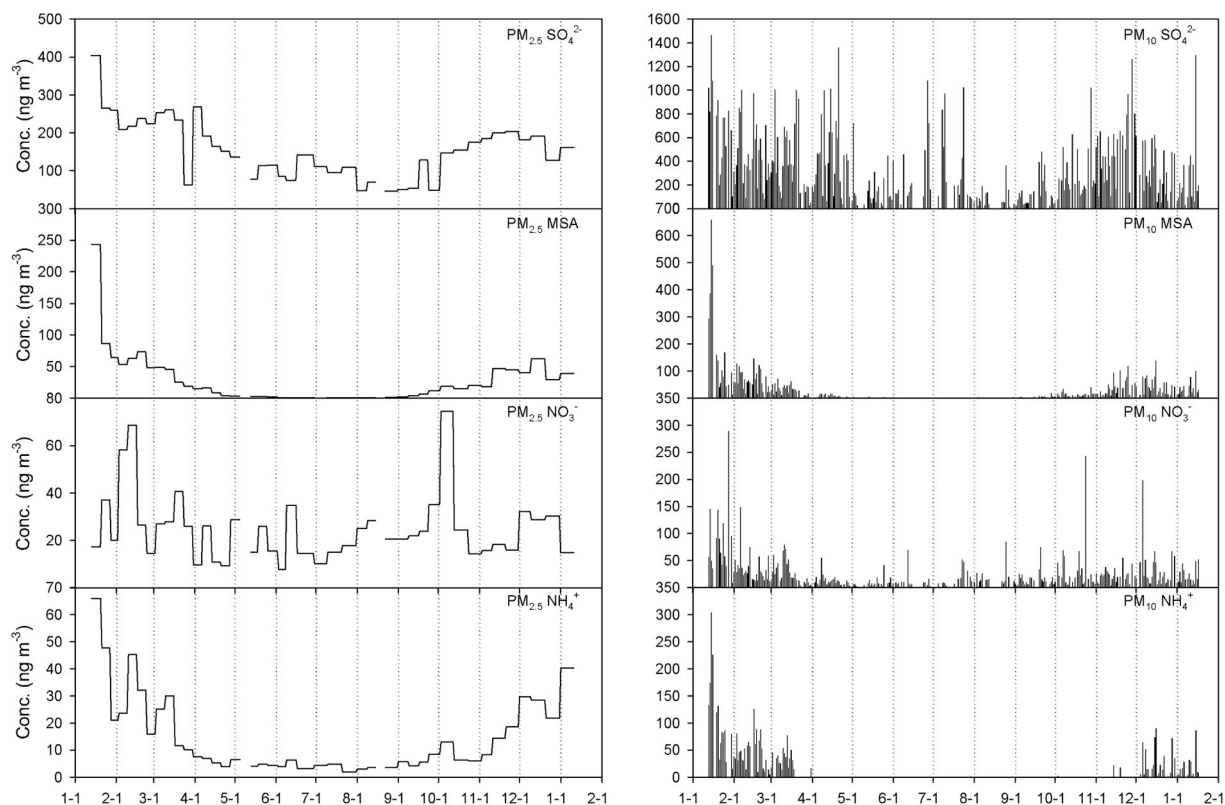


Fig. 2. Concentration variations of MSA ( $\text{CH}_3\text{SO}_3^-$ ),  $\text{NO}_3^-$ ,  $\text{NH}_4^+$  and  $\text{SO}_4^{2-}$  from  $\text{PM}_{2.5}$  and  $\text{PM}_{10}$ .

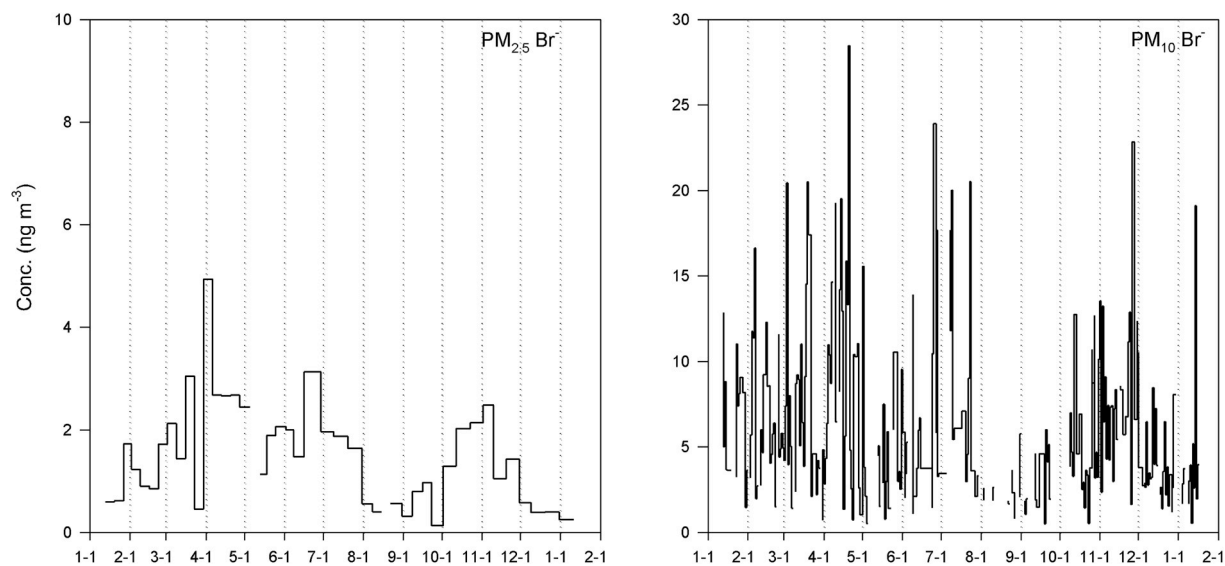


Fig. 3. Concentration variations of  $\text{Br}^-$  from  $\text{PM}_{2.5}$  and  $\text{PM}_{10}$ .

$\text{PM}_{2.5}$  ionic components indicate results from just those particles not affected by the interference of reactive gaseous species on the Teflon filter during each sampling period. With the exception of  $\text{NO}_3^-$ , results indicate a good co-variation between ionic species in  $\text{PM}_{2.5}$  and  $\text{PM}_{10}$ , despite the difference in time resolution. Data from the daily  $\text{PM}_{10}$  sampling clearly show a short term variability of ionic species that the 7-day  $\text{PM}_{2.5}$  data can't provide. Because KSG is very close to the coast, the concentrations of components of sea spray in the ionic components were much higher than those from other sources. Interestingly, the concentration variability of components is definitely different depending on the aerosol formation mechanism, that is, similar variability trends are

evident in ionic species of sea spray and secondary species such as  $\text{CH}_3\text{SO}_3^-$ , nss  $\text{SO}_4^{2-}$  and  $\text{NH}_4^+$ ; but not for  $\text{NO}_3^-$ . Fig. 3 demonstrates that concentration variations of  $\text{Br}^-$  were also very similar to those of ions from sea spray, implying its production process.

Fig. 4 indicates that the distributions of ionic species in  $\text{PM}_{2.5}$  and  $\text{PM}_{10}$  are clearly different depending on the source and formation path of ionic species. For  $\text{PM}_{10}$  sea spray, all 5 cation components are positively skewed (mean > median) indicating that the mean value is substantially influenced by a smaller number of large events (possibly certain days of high wind speed).  $\text{Cl}^-$ ,  $\text{SO}_4^{2-}$  and  $\text{Br}^-$  are all skewed like the sea spray cations, but  $\text{NO}_3^-$  and MSA are even more positively skewed

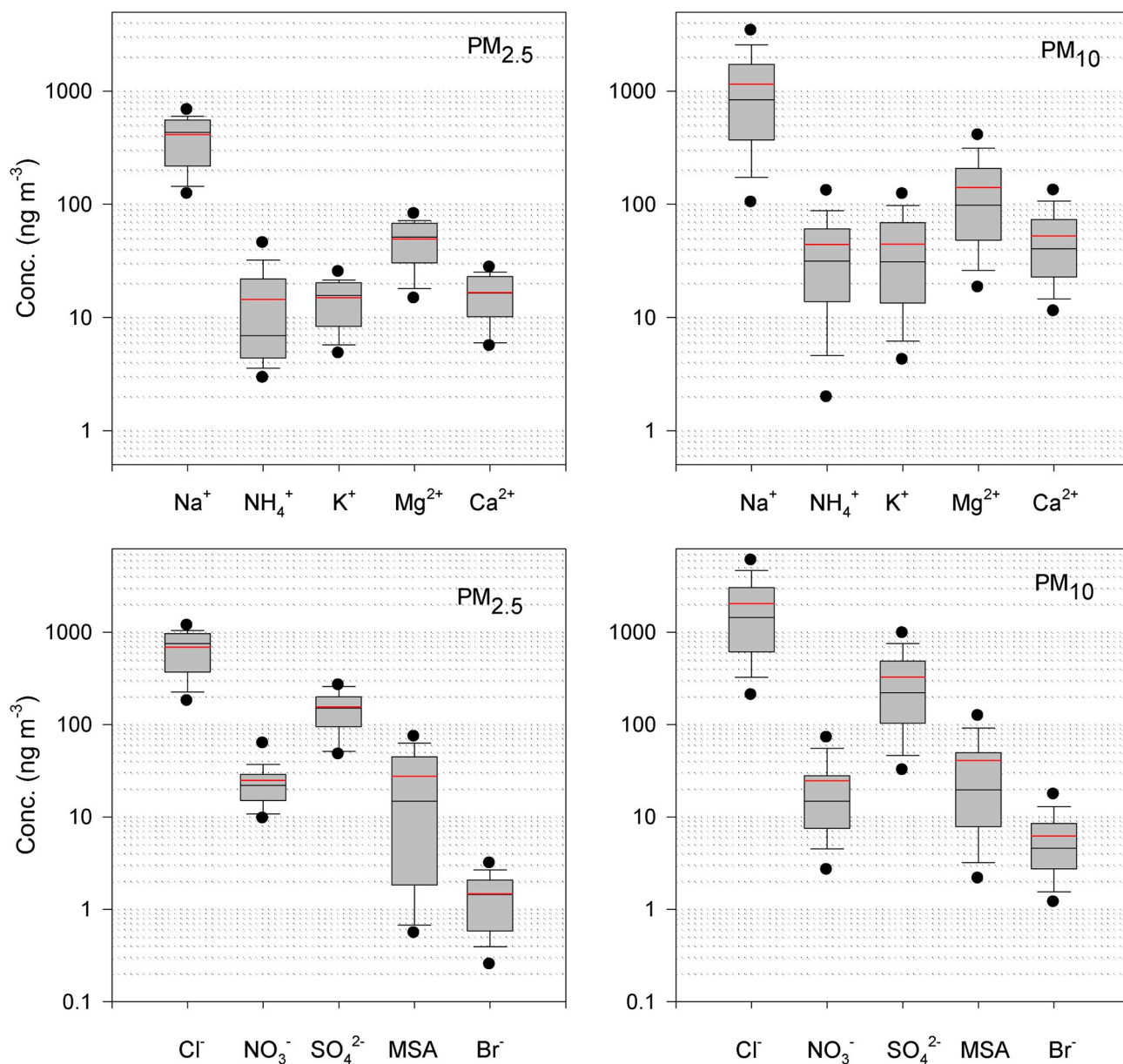


Fig. 4. Concentration distributions of ionic components in  $PM_{2.5}$  and  $PM_{10}$  (25–75%, black line: 50%, red line: mean value, 5–95%, outliers). MSA stands for  $CH_3SO_3^-$ .

(so these are being contributed to by additional occasional large events). For  $PM_{2.5}$ , however, only  $NH_4^+$  is positively skewed (indicating a few large influences – possibly from penguin colony), whereas the other 4 cation components are all normally distributed. MSA is also skewed – so there are probably a few very large events (possibly from algal blooms).

The annual mean concentrations of components from sea spray in  $PM_{10}$  were roughly 3 times higher than those in  $PM_{2.5}$ . The concentrations of  $NH_4^+$  and  $CH_3SO_3^-$  in  $PM_{10}$  are  $\sim 3$  times higher and about the same than those in  $PM_{2.5}$  respectively. This could be due to the data below the detection limit in the daily  $PM_{10}$  series in winter or to the fact that they arise from reactions in the atmosphere and gas to particle conversion processes and are distributed mainly in the finest fraction of the aerosol (Becagli et al., 2011). The  $SO_4^{2-}$  concentration in  $PM_{10}$  is roughly 2 times higher than that in  $PM_{2.5}$  because they also partly exist in the coarse mode after emission from sea salt. Even though annual mean  $NO_3^-$  concentrations in  $PM_{2.5}$  and  $PM_{10}$  are similar, it's more complicated to understand their concentration variations because their correlations were quite weak during the FOP. In this study, as a result,

we focused on the seasonal properties of sea spray, biogenic sulphur and ammonium except for  $NO_3^-$ . A detailed discussion of the concentration variations and source of  $NO_3^-$  will be provided in future publications.

Fig. 5 clearly demonstrates that  $Cl^-$ ,  $Mg^{2+}$ ,  $K^+$ ,  $Ca^{2+}$ ,  $SO_4^{2-}$  and  $Br^-$  were closely correlated with  $Na^+$  in  $PM_{2.5}$  ( $PM_{10}$ ) and, from the slopes of regression lines between them similar to the mean sea water composition, they were mainly expected to originate from sea spray. Interestingly, the slope (0.0045 in  $PM_{10}$  and  $PM_{2.5}$ ) of the regression equation between  $Br^-$  and  $Na^+$  also was a bit lower than the  $Br^-/Na^+$  ratio (0.0062 w/w). Consequently, it is also expected that emission of  $Br^-$  is closely related with the production process of sea spray from marine areas. However, lower  $r^2$  values of best fits and lower slope in  $PM_{2.5}$  indicated possible fractionation processes by chemical reactions in aerosol such as bromine release to the atmosphere from  $Br^-$  in the sea salt aerosol (Vogt et al., 1996).  $SO_4^{2-}$  was also weakly correlated with  $Na^+$  compared to other ions. This weak correlation, which is especially visible in  $PM_{2.5}$ , was ascribed to the additional emission sources as well as sea spray. It has been well established that  $SO_4^{2-}$  in Antarctica is

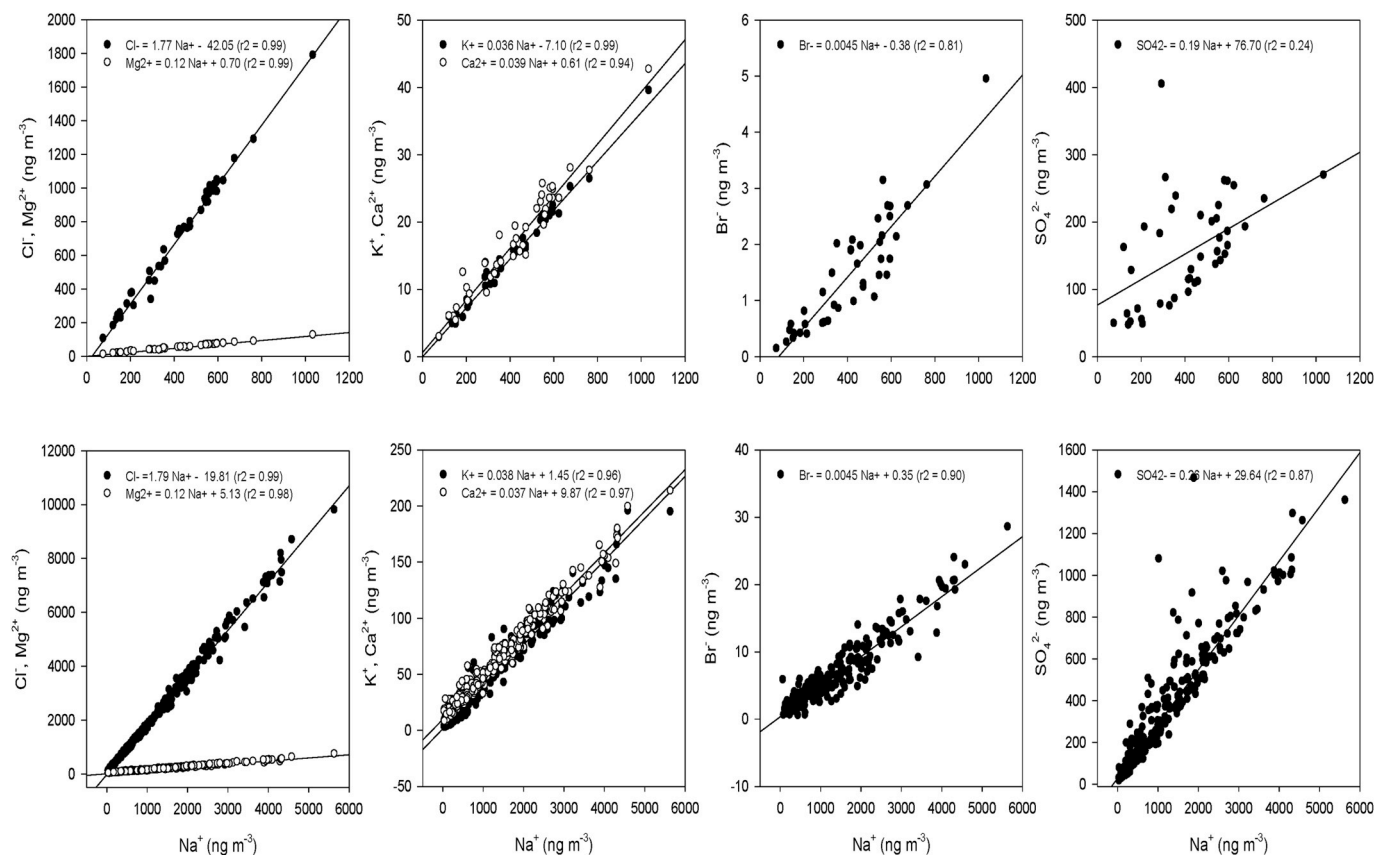


Fig. 5. Regression analyses between ionic components and  $\text{Na}^+$  in  $\text{PM}_{2.5}$  (top) and  $\text{PM}_{10}$  (bottom).

mainly formed as a secondary product from dimethylsulfide (DMS) emitted at ocean surface during spring-summer. Also, it was expected the influence of  $\text{SO}_4^{2-}$  from long-range transport as well as local effect of Antarctic research stations due to location of KSG though their contributions might be very weak (Mishra et al., 2004).

### 3.2. Seasonal variations of mass, ionic compositions, sea spray, sulphur species and ammonium

#### 3.2.1. $\text{PM}_{2.5}$ mass and compositions (w/w) of ionic species in $\text{PM}_{2.5}$

The annual and summer (December, January and February) mean concentrations of  $\text{PM}_{2.5}$  mass are  $2921.2 \pm 1119.7$  and  $2752.7 \pm 960.8 \text{ ng m}^{-3}$ , respectively, and were in the range 740–5700  $\text{ng m}^{-3}$  during the FOP. Even though year-round observations of mass concentrations of atmospheric particles in sub-Antarctic regions are very sparse (Asmi et al., 2018), our results are in the range of other measurement concentrations from KGI summarized by Préndez et al. (2009).

Fig. 6 indicates that  $\text{PM}_{2.5}$  mass showed no seasonal variation during the FOP. The concentration sum of ionic species and  $\text{PM}_{2.5}$  mass were closely correlated, indicating  $\text{PM}_{2.5}$  mass was largely influenced by concentrations of ionic species and thus the concentrations of ionic species can greatly affect  $\text{PM}_{2.5}$  mass. Especially, because the variations of concentrations of sea spray components are closely related with those of the variations of  $\text{PM}_{2.5}$  mass (see Figs. 1 and 6a),  $\text{PM}_{2.5}$  mass variability can be sensitive to the meteorological conditions affecting the advection of sea spray to KSG.

The ratios of concentration sum of ions to  $\text{PM}_{2.5}$  mass (w/w) maintained roughly 50% all year round with no significant seasonal variation. However, the ratios of the components from sea spray and secondary ions to  $\text{PM}_{2.5}$  mass showed clear seasonal variation. In this study, the sea salt fractions and non-sea salt fractions of each ion were calculated using  $\text{Na}^+$  as sea spray marker with an assumption that the

contribution of dust leachable  $\text{Na}^+$  is negligible as follows (Seinfeld and Pandis, 1998);

- 1) [sea salt  $\text{Cl}^-$ ] =  $1.798 \times$  [sea salt  $\text{Na}^+$ ], unit:  $\text{ng m}^{-3}$
- 2) [sea salt  $\text{Mg}^{2+}$ ] =  $0.12 \times$  [sea salt  $\text{Na}^+$ ]
- 3) [sea salt  $\text{K}^+$ ] =  $0.038 \times$  [sea salt  $\text{Na}^+$ ]
- 4) [sea salt  $\text{Ca}^{2+}$ ] =  $0.036 \times$  [sea salt  $\text{Na}^+$ ]
- 5) [sea salt  $\text{SO}_4^{2-}$ ] =  $0.25 \times$  [sea salt  $\text{Na}^+$ ]
- 6) [non sea salt  $\text{SO}_4^{2-}$ ] = [total  $\text{SO}_4^{2-}$ ] - ( $0.25 \times$  [sea salt  $\text{Na}^+$ ])

The sum of concentrations of sea salt spray components ( $\text{Na}^+$ , sea salt  $\text{Cl}^-$ , sea salt  $\text{SO}_4^{2-}$ , sea salt  $\text{Mg}^{2+}$ , sea salt  $\text{K}^+$  and sea salt  $\text{Ca}^{2+}$ ) increased up to almost 50% of  $\text{PM}_{2.5}$  mass from April and was almost consistent until October but decreased down to 30% as summer (December, January and February) approached. The concentration sums of secondary species ( $\text{CH}_3\text{SO}_3^-$ , non sea salt  $\text{SO}_4^{2-}$ ,  $\text{NO}_3^-$  and  $\text{NH}_4^+$ ) increased up to  $\sim 20\%$  during summer even though, interestingly, the major compositions were yet components from sea spray. Also, the concentration sums of sea salt components and secondary species with respect to the total ion sum concentrations ranged from  $\sim 70\%$  (for summer) to  $\sim 100\%$  (for winter) and almost zero (for winter) to  $\sim 40\%$  (for summer), respectively.

#### 3.2.2. Sea spray

Fig. 7 indicates that monthly  $\text{Na}^+$  concentrations (a representative component of sea spray) in  $\text{PM}_{2.5}$  and  $\text{PM}_{10}$ , show similar monthly variations. They were well correlated with each other ( $r^2 = 0.65$ ,  $\text{PM}_{10} = 2.37 \times \text{PM}_{2.5} + 193.73$ ) during the FOP. The concentration ratios of  $\text{Na}^+$  ( $\text{PM}_{2.5}/\text{PM}_{10}$  (w/w)) were in the range of  $\sim 0.20$ – $\sim 0.50$  (summer:  $\sim 0.20$ , winter:  $\sim 0.50$ ), showing a different partitioning of fine and coarse mode in the  $\text{PM}_{10}$  according to season. That is, the relative contribution of  $\text{Na}^+$  in the fine mode was lower for summer than winter.

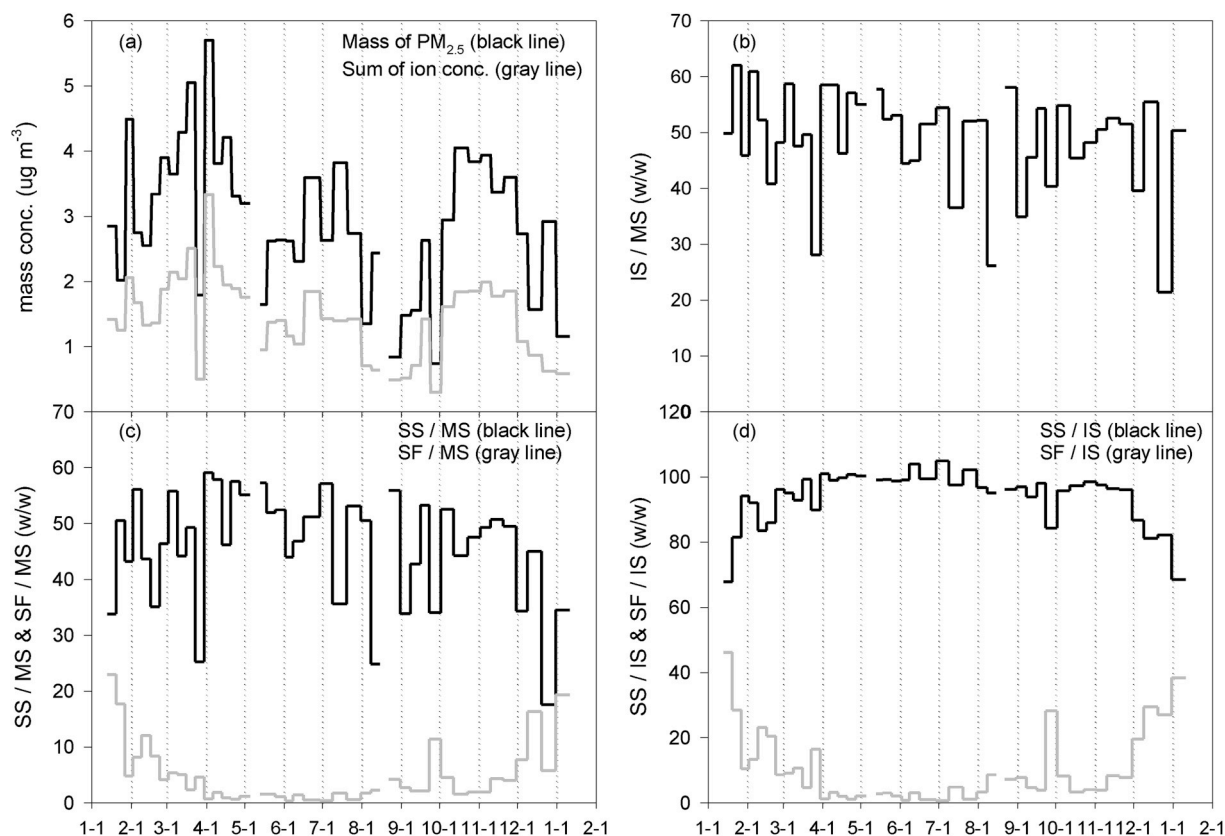


**Fig. 6.** Variabilities of sum of concentrations of ionic components and  $PM_{2.5}$  mass (a), IS/MS (w/w) (b), SS/MS (w/w) and SF/MS (w/w) (c), SF/IS (w/w) and SS/IS (w/w) (d) in  $PM_{2.5}$  (IS: sum of concentrations of ionic species, MS: mass concentrations of  $PM_{2.5}$ , SS: sum of concentrations of sea salt components and SF: sum of concentrations of secondarily species).

This may indicate that different transport paths affect removal efficiency of aerosols, especially, in the coarse mode while they were transported to the measurement site from their source area, and also different emission sources according to season. Interestingly, Legrand et al. (2016) reported a larger presence of submicron sea-salt particles in winter than in summer at DDU, supporting the mechanism of sea-salt aerosol formation via sublimation of blowing salty snow particles during winter season, as formulated in Yang et al. (2008). And thus, sea spray measured at KSG may also be partly originated from sea salt aerosol produced on sea ice area during winter. However, because KGI is located at the marginal sea ice zone of northern tip of Antarctic Peninsula during winter, source emission strength from sea ice area is expected to be much weaker than those of Antarctic coastal area located in high latitude (see Fig. S5). In fact, KGI was partly covered by sea ice since July of 2013 and then totally during August–September. However, the southern ocean is only about 200 km from west to north east of KGI during July–September. As a result,  $\sim 38\%$  of high episodes of  $Na^+$  in  $PM_{10}$  (larger than average value plus standard deviation) during winter just occurred in air masses passing sea ice area.

Of ionic species from sea spray, those other than  $Cl^-$  and  $Br^-$  can be well conserved in the particle phase after emission from their source regions.  $Cl^-$  and  $Br^-$  concentration variations can be influenced by the reaction of  $Cl^-$  and  $Br^-$  in the particle phase and acidic gaseous species because  $Cl^-$  and  $Br^-$  in the particle phase can escape as  $HCl$  (g) and  $Br_2$  (g) during transport (Carmichael et al., 1997; Vogt et al., 1996). However, even if maximum loss of chlorine and bromine occurred (up to  $\sim 20\text{--}35\%$  of sea salt  $Cl^-$  and  $\sim 70\%$  of sea salt  $Br^-$ ) in summer, this would not greatly affect their temporal variations (Fig. S6).

Fig. 7 indicates that  $Na^+$  concentrations in  $PM_{2.5}$  ( $PM_{10}$ ) during the FOP showed no clear seasonal variations, generally higher during April, July and November than those for other months. They indicated a

highest value during fall (March–May) and a lowest value during winter (June–August). Its concentrations during summer (November–April) and winter (May–October), classified by Wagenbach et al. (1998) with the seasonal window selected by the occurrence of sea water  $SO_4^{2-}$  depletion, also indicated that  $Na^+$  levels in  $PM_{2.5}$  ( $PM_{10}$ ) during summer are  $\sim 1.1$  ( $\sim 1.7$ ) times higher than those during winter (Table S3).

Previous studies reported in detail seasonal variations of sea spray for Antarctic regions (Savoie et al., 1993; Wagenbach et al., 1998). They reported no seasonal cycle of  $Na^+$  in TSP at Marsh ( $62^\circ S$ ) and Palmer ( $65^\circ S$ ) because strong  $Na^+$  peaks occurred through the year at both sites. In case of sites located at coastal Antarctica regions, weak seasonal variations of winter maximum and summer minimum at Mawson ( $68^\circ S$ ), Neumayer ( $70^\circ S$ ) and Halley bay ( $75^\circ S$ ) except for DDU ( $66^\circ S$ ), showing summer maximum due to local sea spray, have been reported.

A well-known route of sea spray formation in Antarctic regions is bubble bursting on the open ocean surface (Monaghan et al., 1986). Furthermore, the blowing of frost flowers and snow on sea ice has been also suggested (Rankin et al., 2002; Yang et al., 2008). Wind speed can play a crucial role in enhancing both sea salt generation mechanisms (Prijiith et al., 2014). The transport efficiency from source region to measurement site is also an important factor, particularly in the case of transport of coarse mode sea spray, which is sensitive to the local topography of the measurement site. Consequently, concentration variations of sea spray at KSG might be affected by both the local wind strength and the transport pathway, if it intersects with nearby hills and glaciers.

Fig. 8a indicates that  $Na^+$  concentration in  $PM_{2.5}$  exhibited a degree of correlation with wind speed, the main exceptions being in June–July 2013. Overall the weak correlation during the FOP had an  $r^2 = 0.38$  (Fig. 8b). It was expected that correlation coefficient between daily wind speed and daily  $Na^+$  ( $PM_{10}$ ) would increase because an episode of high

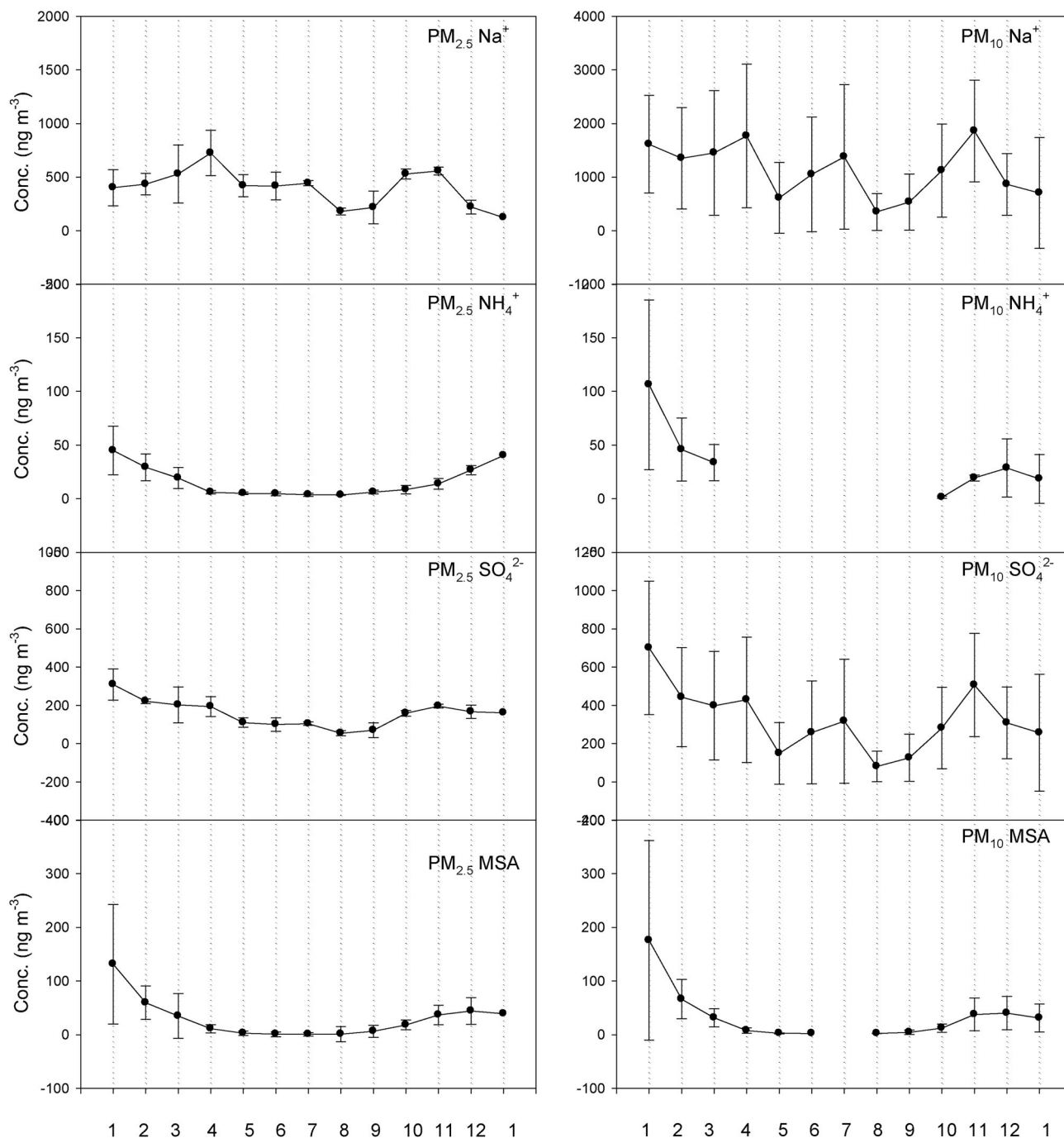


Fig. 7. Monthly concentration (mean  $\pm$  S.D.) variations of major species from  $PM_{2.5}$  and  $PM_{10}$ .

wind speed affecting sea spray loading could be intense but short in time (1 or 2 days). However, there was no correlation between them ( $r^2$ : 0.028 for the FOP, 0.086 for January–February, 2013, 0.024 for March–May, 0.019 for June–August, 0.015 for September–November, 0.025 for December 2013–January 2014). Similarly, correlation between daily sea level pressure (SLP) and  $Na^+$  ( $PM_{10}$ ) were investigated but also, as for the individual data points, no correlation between them during the FOP.

Even though daily  $Na^+$  in  $PM_{10}$  were not correlated with WS and SLP during the FOP, Fig. 8c also indicates that high loading of sea spray episodes in the atmosphere were generally related with high WS and low pressure system associated with storminess. Interestingly, however, daily  $Na^+$  in  $PM_{10}$  also shows their concentrations are likely to be lower under northeasterly and easterly winds although WS is high, especially,

during May–August. This therefore indicates that  $Na^+$  concentrations in aerosols of the atmosphere of KSG might be ascribed to the combined effect of WS (or SLP) and wind direction (WD). Hall et al. (1998) reported that, at Halley station, sea-salt loadings are not linked to high wind speed, but more moderate ones and the high sea-salt loadings are associated with a change in wind direction that opens up an area of water and then switches to bring sea-salt inland. Weller et al. (2008) also reported that there was no correlation between  $Na^+$  concentrations with sampling intervals of 7 day (or 1 day) and wind velocity, and pointed out the importance of the efficiency of the transport process, removal by wet deposition and sea-ice cover.

The monthly variation of wind speed during the FOP indicated that mean wind speeds were comparable throughout the whole summer ( $7.45 \pm 1.62 \text{ m s}^{-1}$  from November to April) and winter ( $8.46 \pm 0.79 \text{ m}$

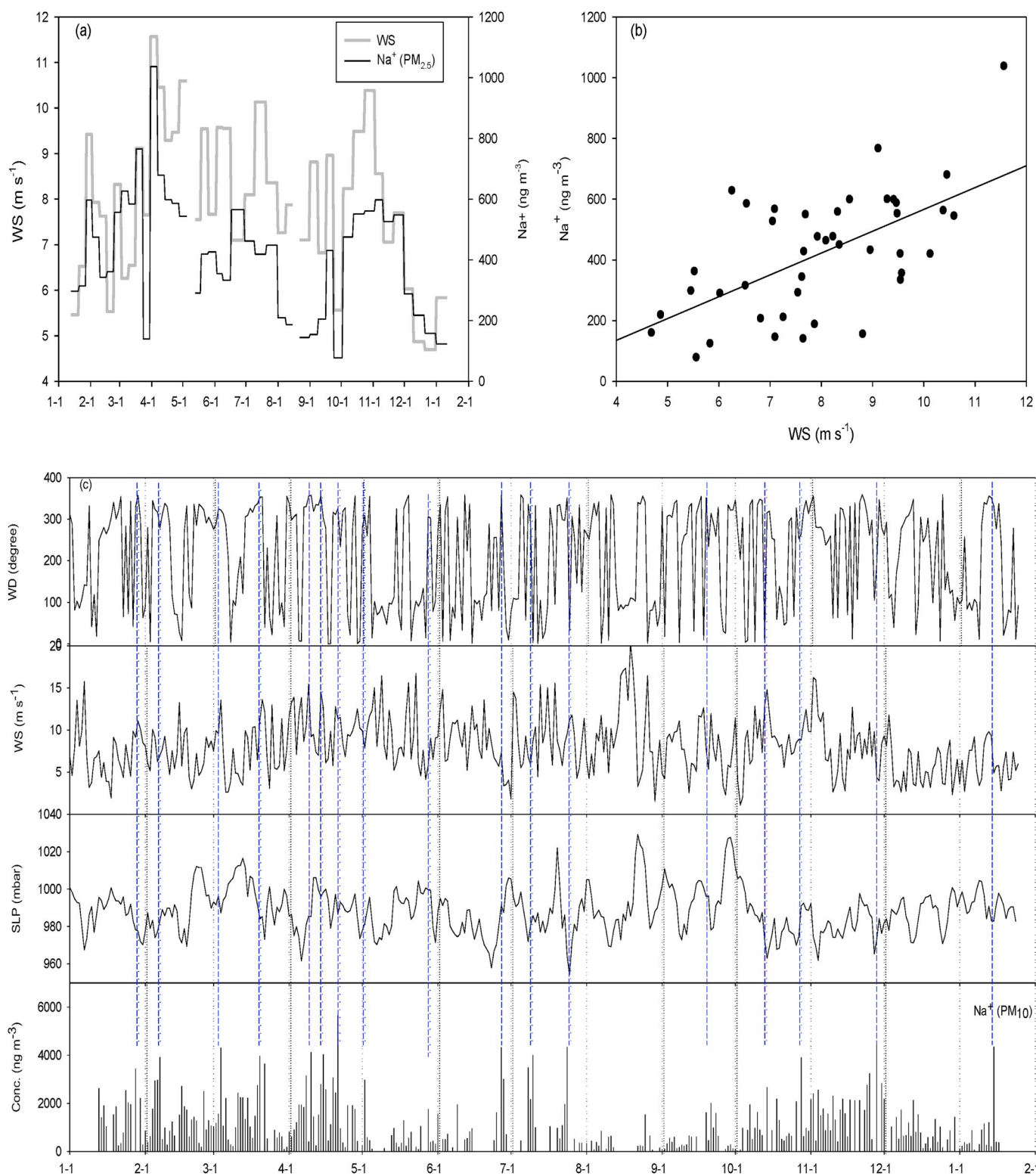


**Fig. 8.** Variabilities of  $\text{Na}^+$  concentrations in  $\text{PM}_{2.5}$  & wind speed (WS) during the FOP (a), Scatter plots between WS and  $\text{Na}^+$  in  $\text{PM}_{2.5}$  (b) (WS was averaged during  $\text{PM}_{2.5}$  sampling periods, PM samplers were unwillingly stopped due to inclusion of snow grains into air inlet impactor during snow storm events as follows; 5/6–10, 6/16–24, 6/30–7/5, 7/12–18 and 8/13–22), and Variations of wind direction (WD), wind speed (WS), sea level pressure (SLP) and  $\text{Na}^+$  in  $\text{PM}_{10}$  (c). Vertical dotted lines (blue) indicate high episode events ( $>$ average plus standard deviation;  $\sim 2700 \text{ ng m}^{-3}$  during Nov–Apr,  $\sim 1700 \text{ ng m}^{-3}$  during May–Oct) of  $\text{Na}^+$  in  $\text{PM}_{10}$  during the FOP.

s<sup>-1</sup> over May–October). That is, the wind speed at KSG was not well defined to show winter maximum during the FOP. This may partly result in relatively similar concentrations of sea spray at KSG during summer and winter, contributing to the weakening of its seasonal cycle.

Fig. 9 presents wind roses at KSG showing monthly variation of wind speed and direction throughout the FOP. Wind directions from west and northwest were prevalent from January to April 2013, after which the frequencies of winds from the east clearly increased from May to August. The wind direction returned again mainly to north westerly during spring but easterly winds increased again in January 2014, in contrast to wind conditions experienced in the summer of 2013. Maxwell Bay lies to

the west of KSG, and mountain glaciers with elevations of ~300 m and ~600 m are found to the east and northeast of KSG, respectively. Therefore, the transport efficiency of sea spray to the AOB at KSG might be different according to the specific approach path. It is expected that sea spray is transported to KSG quite efficiently under wind directions from south to northwest, but less so in the case of northerly to easterly winds passing over the mountain glacier area.

### 3.2.3. Sulphur species

CH<sub>3</sub>SO<sub>3</sub><sup>-</sup> and SO<sub>4</sub><sup>2-</sup> concentrations during the FOP exhibited a clear seasonal cycle, characterised by an austral summer maximum and

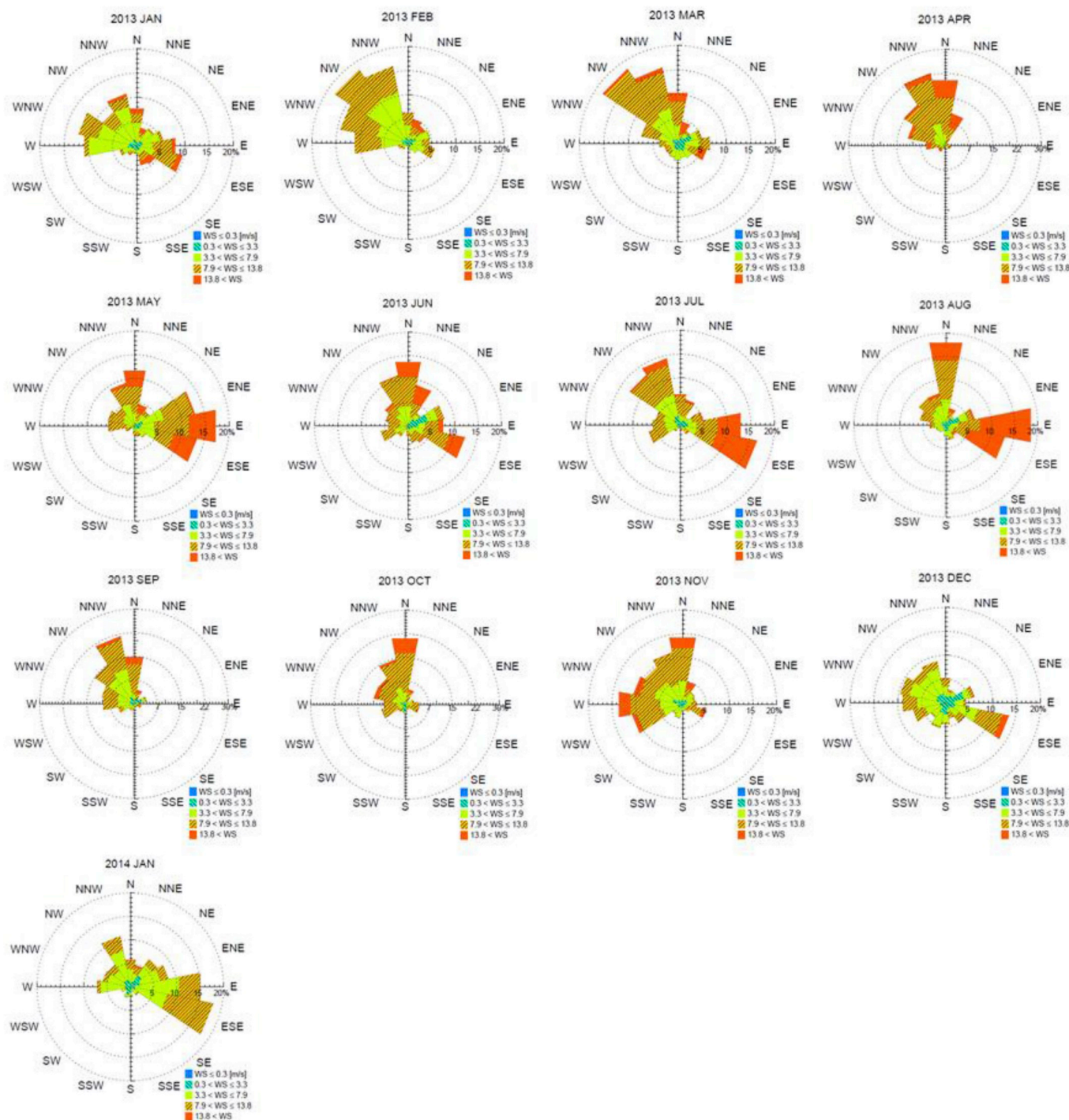
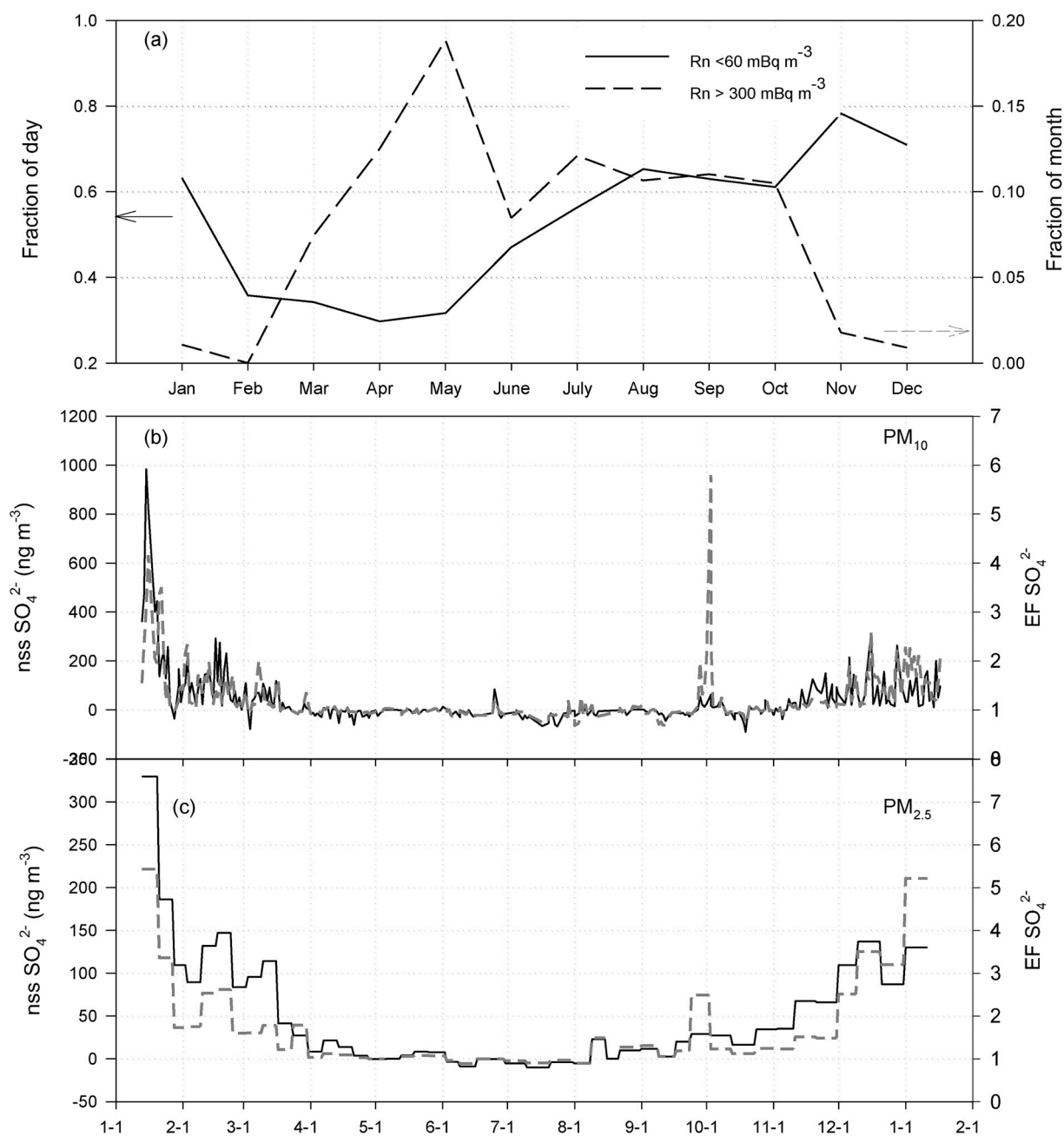


Fig. 9. Monthly variations of wind rose patterns during the FOP.

austral winter minimum (see Fig. 7 and Table S3).  $\text{CH}_3\text{SO}_3^-$  concentration in  $\text{PM}_{2.5}$  ( $\text{PM}_{10}$ ) during summer (November–April) is 7 (10) times higher than those during winter (May–October).  $\text{SO}_4^{2-}$  concentration also is 2 times higher in both  $\text{PM}_{2.5}$  and  $\text{PM}_{10}$  during summer.

Seasonal cycles of  $\text{CH}_3\text{SO}_3^-$  and nss  $\text{SO}_4^{2-}$  in aerosols and snow in Antarctica have previously been reported, and their production processes investigated (Davis et al., 1998). Even though nss  $\text{SO}_4^{2-}$  in the Antarctic atmosphere partly originates from  $\text{SO}_2$  from volcanic eruptions, the emission source of  $\text{CH}_3\text{SO}_3^-$  is primarily from DMS emitted by algae in the ocean area. Importantly, the concentration of  $\text{CH}_3\text{SO}_3^-$  was positively correlated with the concentration of nss  $\text{SO}_4^{2-}$  during summer of FOP ( $r^2 = 0.87$ ). Therefore, increments of nss  $\text{SO}_4^{2-}$  and  $\text{CH}_3\text{SO}_3^-$  concentrations during summer are likely attributable to DMS emission strength from the source area and transport efficiency of air mass.

As a source of nss  $\text{SO}_4^{2-}$  in aerosol measured at KSG, however, the long-range transport from South America and local impact from Antarctic research stations might also be possible and their effects to variations of nss  $\text{SO}_4^{2-}$  need to be investigated. In this study, based on  $^{222}\text{Rn}$  gas (Fig. 10a), which is atmospheric tracer of recent terrestrial influence, from November–February there are mainly local influences at KSG, but March/April and September/October are times of common transport of air masses from South America. Fig. 10a showed that in summer (November–February) there are almost no radon contributions from South America (radon gas concentrations  $> 300 \text{ mBq m}^{-3}$ ), and there are also few in June. However, in other months, from March to October there are on average 5 days a month when radon gas comes from South America (and other chemicals). Fig. 10a also indicated the distribution of how many hours each day (for a monthly composite day) are in



**Fig. 10.** Fraction of day that hourly  $\text{Rn} < 60 \text{ mBq m}^{-3}$  (baseline) and Fraction of month that daily  $\text{Rn} > 300 \text{ mBq m}^{-3}$  (a), nss  $\text{SO}_4^{2-}$  (black, straight line) and enrichment factor values of  $\text{SO}_4^{2-}$  (gray, dotted line) in  $\text{PM}_{10}$  with respect to sea water composition (b) and nss  $\text{SO}_4^{2-}$  (black, straight line) and enrichment factor values of  $\text{SO}_4^{2-}$  (gray, dotted line) in  $\text{PM}_{2.5}$  with respect to sea water composition (c).

“baseline” conditions (radon gas concentrations  $< 60 \text{ mBq m}^{-3}$ ). For February to May, more than half of every day of the month (on average) has radon concentrations  $> 60 \text{ mBq m}^{-3}$  (“baseline”), but only in March, April and May are these likely to have come from South America.

Enrichment factor (EF) values of  $\text{SO}_4^{2-}$  with respect to sea water composition were calculated in order to investigate contribution of sources other than sea spray (Fig. 10b–c). EF values of  $\text{SO}_4^{2-}$  in  $\text{PM}_{2.5}$  were consistently in the range of 0–1 and also nss  $\text{SO}_4^{2-}$  were negative values during May–July, showing the existence of mirabilite precipitated when the sea ice is formed during winter (Wagenbach et al., 1998). EF values of  $\text{SO}_4^{2-}$  and nss  $\text{SO}_4^{2-}$  in  $\text{PM}_{10}$  also showed similar trends as those of  $\text{PM}_{2.5}$  but occasionally from the middle of March to October, abrupt increment of EF values of  $\text{SO}_4^{2-}$  over unity during short periods of winter was shown. They were mostly in the range of 1–2 and clearly increased up to  $\sim 5.5$  on 2–4th, October though their concentrations are very low. These suggest that other sources such as long-range transport from continental region and research stations, even though trace elements should be measured to clarify them, can affect variations of nss  $\text{SO}_4^{2-}$  in aerosol of the KSG atmosphere but their effect might be insignificant.

Interestingly,  $\text{CH}_3\text{SO}_3^-$  and  $\text{SO}_4^{2-}$  concentrations during January of 2013 were roughly 2–3 times higher than those during other months of summer of the FOP. Concentration variability of secondary species in

sampled aerosols can be influenced by photochemistry and meteorology. In order to investigate the photochemical activity in the atmosphere in the summers of 2013 and 2014, the relevant meteorological parameters (air temperature and total solar radiation) were compared. Temperature characteristics in January 2013 and 2014 were very similar, in the range of  $-2.4$  to  $6.5 \text{ }^\circ\text{C}$  (average:  $0.8 \text{ }^\circ\text{C}$ ) and  $-3.8$  to  $7.0 \text{ }^\circ\text{C}$  (average:  $0.8 \text{ }^\circ\text{C}$ ), respectively. The corresponding intensities of total solar radiation were  $378216$  and  $510528 \text{ kJ m}^{-2}$ , respectively. Therefore, photochemical processing was expected to be more active in January 2014. The lower concentrations in January 2014 indicate that photochemistry is not a critical factor to influence the concentrations of  $\text{CH}_3\text{SO}_3^-$  and nss  $\text{SO}_4^{2-}$  for these two months. The atmospheric mixing heights in January for 2013 and 2014, which can affect concentrations of atmospheric components, were almost the same;  $124$ – $827 \text{ m}$  (average:  $\sim 474 \text{ m}$ ) in January 2013 and  $118$ – $750 \text{ m}$  (average:  $\sim 496 \text{ m}$ ) in January 2014 (<http://www.ready.noaa.gov/ready>).

Potential source regions and strengths of DMS emissions, as well as air mass transport pathways to the measurement site, can influence observed sulphur species concentrations at KSG. Consequently, surface water phytoplankton concentrations, and sea ice concentrations as well as clustered 3-day air mass back-trajectories (Fig. 11) were investigated. Results indicated that sea-surface chlorophyll concentration in the Bellingshausen Sea area, as well as the transport pathways of air masses

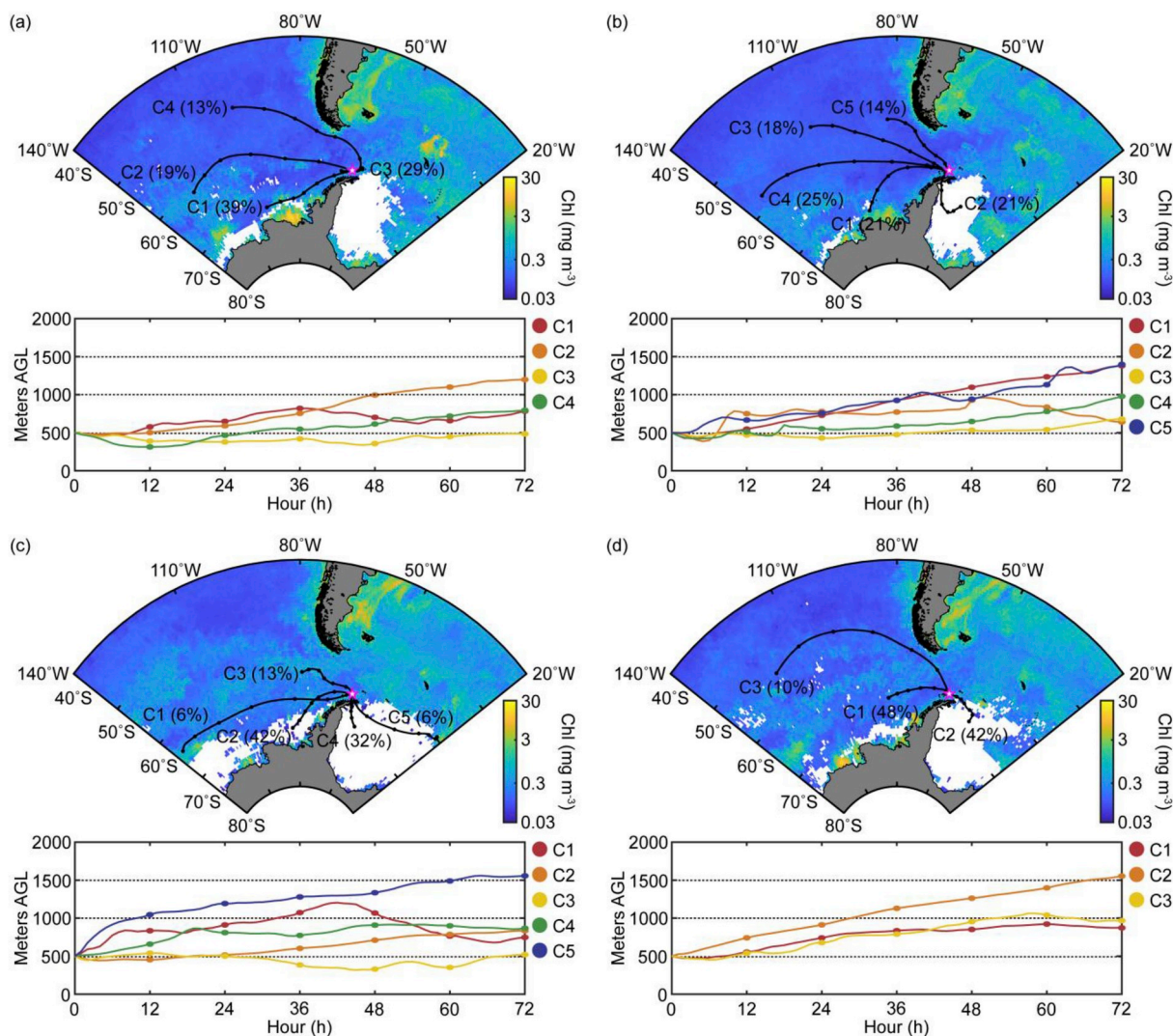


**Fig. 11.** Clustered 3-day back trajectories, chlorophyll-a and sea ice area during January 2013 (a), February 2013 (b), December 2013 (c) and January 2014 (d) for King Sejong Station during the FOP (Lower panels indicate air mass elevation).

approaching KSG, were significantly different in the summers of 2013 and 2014.

It has been well established that DMS emission strength is closely related to phytoplankton biomass in surface seawaters (Park et al., 2013, 2018; Jung et al., 2014), and that phytoplankton is prevalent in the marginal zone of sea ice as it begins to melt, as well as in polynya regions (Zhang et al., 2015). A recent study revealed that DMS-induced new particle formation occurred more intensively for air masses originating from the Bellingshausen Sea than those of Weddell Sea owing to higher abundance of DMS-rich phytoplankton in the Bellingshausen Sea than in the Weddell Sea during the austral summer period (Jang et al., 2019).

Fig. 11a shows that a significant algae bloom occurred in the Bellingshausen Sea area ( $\sim 80\text{--}95^\circ\text{W}$ ,  $\sim 70\text{--}74^\circ\text{S}$ ), west of the Antarctic Peninsula, in January and February of 2013. Chlorophyll-*a* concentrations in January of 2013 were  $\sim 1.5\text{--}2$  times higher than those in either February of 2013 or January of 2014. It is interesting to note that the distribution of sea ice in the Bellingshausen Sea was also clearly different between summer of 2013 and 2014 (Fig. S5), which also shows a close relationship between algae bloom and sea ice coverage. Air masses frequently arrived at KSG after having passed over these potential areas of high DMS emission (cluster 1 from Fig. 11a and 11b) but Fig. 11b also indicated that the cluster 1 group of air masses during February of 2013 clearly decreased and the cluster 2 group of air masses having passed sea ice covered area increased, thus causing lower concentrations of sulphur species in aerosol than those during January of 2013.

By comparison, the algae bloom area was definitely smaller in the summer of 2014, indicative of a weak DMS emission intensity. The clustered 3-day air mass back-trajectories of Fig. 11c and d clearly show that the frequency of wind moving to KGI after passing regions of algal blooming also decreased, in favour of more easterly winds. A combination of these factors is expected to have led to the higher concentrations of biogenic sulphur species in  $\text{PM}_{2.5}$  ( $\text{PM}_{10}$ ) collected at KSG in summer of 2013 than in summer of 2014.

### 3.2.4. Ammonium

$\text{NH}_4^+$  concentration in  $\text{PM}_{2.5}$  ( $\text{PM}_{10}$ ) during summer (November–April) is  $\sim 5$  (35) times higher than those during winter (May–October) (Table S3).  $\text{NH}_4^+$  concentration variations were relatively well correlated with those of  $\text{CH}_3\text{SO}_3^-$  and  $\text{SO}_4^{2-}$  during the FOP (Fig. 7). In particular,  $\text{NH}_4^+$  concentration was clearly higher during the middle of January 2013 as were the concentration trends of  $\text{CH}_3\text{SO}_3^-$  and  $\text{SO}_4^{2-}$  even if its increment factor is not higher than those of  $\text{CH}_3\text{SO}_3^-$  and  $\text{SO}_4^{2-}$  (Fig. 2).

The potential source area and transport efficiency should be investigated to figure out seasonal variations of  $\text{NH}_4^+$  in aerosols. Also  $\text{NH}_3$ , which is a precursor of  $\text{NH}_4^+$  in the aerosol phase, concentration variations can be an important factor because  $\text{NH}_4^+$  is formed through neutralization reaction with acidic species. Previous studies have suggested  $\text{NH}_3$  is mainly released from biological activity in marine areas and penguin colony area in the Southern Ocean and Antarctica. The role of penguin colonies and the Southern Ocean to influence concentrations of  $\text{NH}_3$  (g)/ $\text{NH}_4^+$  (p) in the Antarctic atmosphere was previously investigated at DDU (Legrand et al., 1998). They found that  $\text{K}^+$  and  $\text{Ca}^{2+}$  in aerosol was clearly enriched relative to the sea water composition, and oxalate concentrations definitely increased in cases where the measurement site was directly affected by ornithogenic soil particle emitted from the penguin colony area. However, interestingly, even if the site such as Ile du Gouverneur site was just  $\sim 2.5$  km away from main penguin colony, the compositions of  $\text{K}^+$  and  $\text{Ca}^{2+}$  to  $\text{Na}^+$  were almost same as those of sea water and oxalate concentration was also very low, indicating the rapid decrease of direct influence from penguin colony area. However, the concentration of  $\text{NH}_3$  (g) in the atmosphere was still high.

Therefore, based on clear seasonal variations and strong correlation with  $\text{CH}_3\text{SO}_3^-$  ( $r^2 = 0.68$ ) and nss  $\text{SO}_4^{2-}$  ( $r^2 = 0.91$ ) during summer

(November–April), firstly, the source of  $\text{NH}_4^+$  is expected to be closely related with those of  $\text{CH}_3\text{SO}_3^-$  and nss  $\text{SO}_4^{2-}$ . Savoie et al. (1993) reported the primary source for the  $\text{NH}_4^+$  might be the same as for  $\text{CH}_3\text{SO}_3^-$ , i.e. biological activity in the Southern Ocean at Palmer and Mawson Station using the similarities of their concentration variabilities.

Secondly, a potentially important factor affecting  $\text{NH}_4^+$  concentration variations in atmospheric aerosols in the KGI area is penguin colonies. It has been well established that penguins can affect ammonia ( $\text{NH}_3$ ) concentration in the Antarctic atmosphere near their breeding areas, which are mainly located in coastal regions of Antarctica (Legrand et al., 1998). Because KGI is recognised as being one of the more densely populated penguin areas (due to the protection zones), it is expected that  $\text{NH}_3$  concentrations are also generally higher in summer than in winter due to changes in emission intensity from penguin colonies.

Fig. 12 shows  $\text{K}^+$  and  $\text{Ca}^{2+}$  enrichment factors relative to sea water composition were  $\sim 1\text{--}2$  in January 2013, with similar values also in other periods, indicating a primarily sea spray origin. Oxalate was not consistently measured in the summer of the FOP, only for  $\text{PM}_{10}$  in early October 2013. The  $\text{NH}_3$  concentrations were much higher in the summer of 2013 and closely correlated with  $\text{NH}_4^+$  ( $r^2 = 0.87$ , on a molar basis,  $[\text{NH}_4^+] = 0.13 [\text{NH}_3] - 0.00$ ) even if no correlation between  $\text{NH}_3$  (g) and  $\text{NH}_4^+$  (p) was found during the summer of 2014. Therefore,  $\text{NH}_4^+$  in aerosol sampled at KSG during the summer of 2013 might not be directly influenced by ornithogenic soil particles suspended in the atmosphere of the penguin colony areas near KSG despite their close proximity, but rather be secondarily products formed in the atmosphere from  $\text{NH}_3$ .

$\text{NH}_4^+$  concentrations in  $\text{PM}_{10}$  ( $\text{PM}_{2.5}$ ) and  $\text{NH}_3$  concentration are  $\sim 48.6 \pm 52.5$  ( $\sim 33.8 \pm 14.8$ ) and  $237.7 \pm 140.5$   $\text{ng m}^{-3}$  in austral summer (December, January, and February), showing the  $\text{NH}_3$  concentrations are  $\sim 5\text{--}8$  times higher than those of  $\text{NH}_4^+$  in  $\text{PM}_{10}$  ( $\text{PM}_{2.5}$ ). These results indicated  $\text{NH}_4^+$  in  $\text{PM}_{10}$  and  $\text{NH}_3$  concentrations in summer are 50% lower than those reported for Ile du Gouverneur ( $\text{NH}_4^+$ : 102,  $\text{NH}_3$ : 530  $\text{ng m}^{-3}$ ) (Legrand et al., 1998) but, interestingly, similar concentration distributions in gas and particle phase between two sites.

During the summer of 2013, based on the correlation analysis between  $\text{NH}_3$  and  $\text{NH}_4^+$  and their distribution in gas and particle phase,  $\text{NH}_3$  in the atmosphere of KSG could directly take part in the acid-base chemistry and thus influence concentration variabilities of  $\text{NH}_4^+$  in aerosol. Also acidic species in aerosols would play a role as a limiting factor to neutralize  $\text{NH}_3$  in the atmosphere because  $\text{NH}_3$  concentration is much higher.

Fig. 12 indicated that  $\text{NH}_3$  concentrations during summer of 2014 were in the range of about 10–50% lower than during summer of 2013. The driving factors to cause the observed increase of  $\text{NH}_3$  concentrations in January to February 2013 should also be investigated. Because total microalgal biomass (total chlorophyll *a* concentration) observed in the sea water sampled at the port of KSG were similar during the summer of 2013 and 2014 (Choi, 2014), the process of biological degradation of uric acid from penguin colony area might be more important. It has been known that the uric acid degradation in fresh penguin excreta is affected by soil temperature and moisture, enzyme activity and soil moisture is known to be a main factor (Legrand et al., 1998). Of meteorological parameters measured at KSG, which are closely related with the soil temperature and moisture, the ambient temperature was similar but, precipitation amount was clearly different. They were  $\sim 88$  and 99.6 mm on January and February of 2013 but 9.8 and 5.6 mm on December of 2013 and January of 2014. Therefore, as soil moisture is expected to be higher, the release of  $\text{NH}_3$  from penguin breeding areas might be more efficient during summer of 2013.

Furthermore, the wind direction during summer of 2013 and 2014 changed from northwest to east (Fig. 9). Especially, during summer of 2014, the air mass mainly moved to KSG over mountain glaciers from the Weddell Sea sector (Fig. 11c and d). Considering the location of penguin protection areas of KGI with respect to the wind direction and biological activity in the ocean area surrounding KGI,  $\text{NH}_3$  emitted from source areas have little effect in the summer of 2014. Furthermore,  $\text{NH}_3$

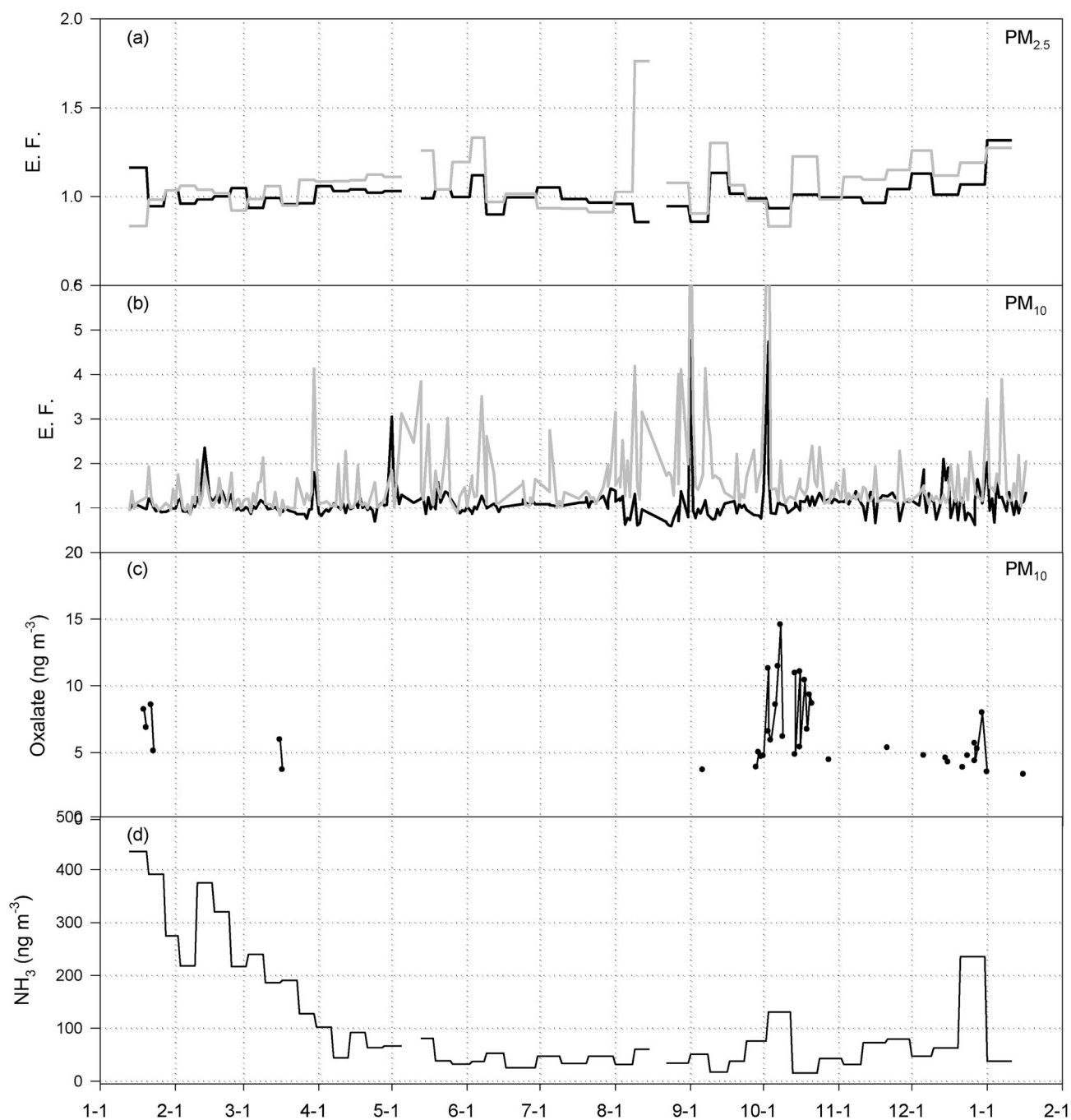


**Fig. 12.** Temporal variations of enrichment factor (E.F.) values of  $\text{K}^+$  (black line) and  $\text{Ca}^{2+}$  (gray line) in  $\text{PM}_{2.5}$  (a) and  $\text{PM}_{10}$  (b), oxalate ion concentrations in  $\text{PM}_{10}$  (c) and  $\text{NH}_3(\text{g})$  from denuder tube during the FOP (d) (Penguins left at the ASPA 171 of Baton Peninsula on the middle of April 2013, and again appeared at ASPA 171 on ~ 21st Oct 2013).

might not be transported efficiently over mountain glaciers because the atmospheric mixing height is sometimes lower than the elevation of the mountain glaciers. Consequently, strong emission of  $\text{NH}_3$  as well as transport path of air masses all might drive much higher concentration of  $\text{NH}_3$  during summer of 2013 than 2014.

Considering the residence time (~a few hours) of  $\text{NH}_3$  in the atmosphere of KSG ( $62^\circ$  south), sub Antarctic (Norman and Leck, 2005) and clearly higher concentrations during summer of 2013, the concentration of  $\text{NH}_3$  of KSG atmosphere might be controlled by local emission source. As major sources of  $\text{NH}_3$  of KSG atmosphere during summer, release from biological decomposition of uric acid from penguin colony areas of KGI as well as biological activity in the ocean near KGI can contribute

higher concentration of  $\text{NH}_3$  of KSG atmosphere than those during winter. While they both have some potential to influence the general increase in summer, however, in this study, it's difficult to clarify relative contribution of these emission sources to affect the concentration variability of  $\text{NH}_3$  sampled at KSG atmosphere. In fact, we need to measure  $\text{NH}_3(\text{g})/\text{NH}_4^+(\text{p})$  in the area of penguin colony and ocean area surrounding KSG during summer.

Fig. 13 shows the possibility of  $\text{NH}_4^+$  formation in  $\text{PM}_{2.5}$  by the reaction between basic gaseous  $\text{NH}_3$  and acidic gases ( $\text{H}_2\text{SO}_4$ ,  $\text{CH}_3\text{SO}_3\text{H}$  and  $\text{HNO}_3$ ). The slopes (~2.23 and ~1.31) of the regression lines, which are over unity, between  $\text{NH}_4^+$  and  $\text{CH}_3\text{SO}_3^-$  plus  $\text{nss SO}_4^{2-}$  really indicates that both  $\text{CH}_3\text{SO}_3^-$  and  $\text{nss SO}_4^{2-}$  also can originate from cation related

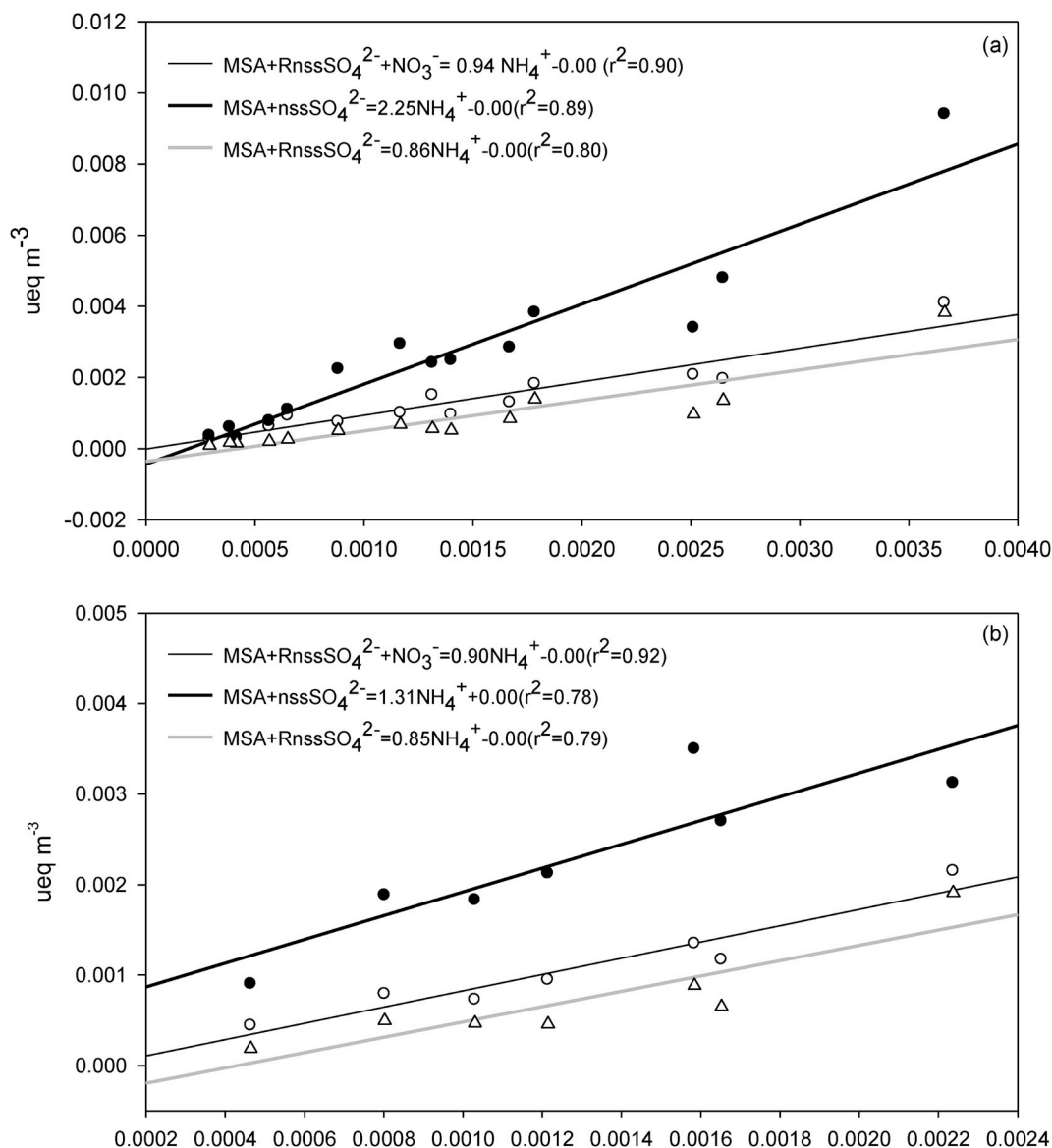


**Fig. 13.** Regression analyses between  $\text{NH}_4^+$  and  $\text{MSA} + \text{nssSO}_4^{2-}$  (black thick line),  $\text{MSA} + \text{RnssSO}_4^{2-}$  (gray line),  $\text{MSA} + \text{RnssSO}_4^{2-} + \text{NO}_3^-$  (black thin line) in  $\text{PM}_{2.5}$  during January–April 2013 (a) and November 2013–January 2014 (b).  $\text{MSA}$  and  $\text{nssSO}_4^{2-}$  indicates  $\text{CH}_3\text{SO}_3^-$  and non-sea salt sulphate (i.e.,  $\text{SO}_4^{2-}$  minus  $\text{Na}^+ \times 0.251$ ).  $\text{RnssSO}_4^{2-}$  indicates remained non-sea salt sulphate to take part in acid-base atmospheric chemistry with ammonia after reaction of  $\text{NaCl}$  in particle and  $\text{H}_2\text{SO}_4$  (i.e.,  $\text{nssSO}_4^{2-}$  minus the amount of chlorine loss). The amount of chlorine loss during transport was calculated by sea salt  $\text{Cl}^-$  (i.e.,  $\text{Na}^+ \times 1.798$ ) minus  $\text{Cl}^-$ .

salt other than  $\text{NH}_4^+$ . Because  $\text{HCl}$  (g) can escape by the adsorption of acidic gases to sea spray, we assumed the reaction of  $\text{NaCl}$  in sea spray and  $\text{H}_2\text{SO}_4$  produced by  $\text{DMS}$  oxidation reaction takes place in the ocean area during transport (Seinfeld and Pandis, 1998). As a result,  $\text{nssSO}_4^{2-}$  can partly combine with  $\text{Na}^+$  as a  $\text{Na}_2\text{SO}_4$ , not  $\text{NH}_4^+$  in the aerosol phase. After consideration of a chlorine deficit phenomenon like this, the slopes of  $\text{NH}_4^+$  and  $\text{CH}_3\text{SO}_3^-$  plus  $\text{RnssSO}_4^{2-}$  (non sea salt  $\text{SO}_4^{2-}$  from  $\text{H}_2\text{SO}_4$  not to be participated in the chlorine loss reaction) were  $\sim 0.86$  and  $\sim 0.85$  for each summer. They increased up to  $\sim 0.94$  and  $\sim 0.90$  in case  $\text{HNO}_3$  can also be combined with  $\text{NH}_3$ . Therefore, these indicate that  $\sim 85\%$  of  $\text{NH}_3$  was mostly neutralized by acidic sulphur species ( $\text{H}_2\text{SO}_4$  and  $\text{CH}_3\text{SO}_3\text{H}$ ) during summer and  $\text{HNO}_3$  also can contribute to neutralize basic component though it has a minor one. This study shows that  $\text{NH}_3$  other than sea spray, which has been normally known as a base in Antarctica, has played an important role as a basic component in acid-base chemistry of the aerosol sampled at KSG.

#### 4. Summary

Systematic research was conducted in 2013 on the aerosol chemistry at King Sejong Antarctic station located on Barton Peninsula of King George Island, near the northern tip of the Antarctic Peninsula. It is expected that this work will contribute to the understanding of temporal and spatial characteristics of aerosol composition in the Antarctic Peninsula region and thus the role of aerosols to influence ongoing climate variability. This study showed seasonal trends of mass and major ions (sea spray, sulphur species and ammonium) in  $\text{PM}_{10}$ , even though they should be clarified further with multi-year measurements. We suggested possible factors (meteorology, biogenic activity in ocean area and penguin colony) to influence the concentration variabilities of major ions in aerosols during the 1-year field observation period. Results indicated that the ratios of concentration sum of ions to  $\text{PM}_{2.5}$  mass (w/w) maintained roughly 50% all year round with no significant seasonal variation and they were mainly composed of sea spray compounds because of the coastal location of the measurement site, consistently

affected by polar low pressure ( $\sim 62^\circ$  south). Seasonal variability of masses and concentrations of sea spray compounds might be influenced by the topography surrounding measurement site as well as meteorology over the year. Of the secondary species, the concentrations of biogenic sulphur species over summer were affected by both emission intensities of precursor from oceanic algal bloom areas (for example,  $\sim 80\text{--}95^\circ\text{W}$ ,  $\sim 70\text{--}74^\circ\text{S}$  near the Bellingshausen Sea during January and February of 2013) and the frequency of air masses passing over this source area. Based on  $^{222}\text{Rn}$  activities and EF values of  $\text{SO}_4^{2-}$  with respect to sea water composition, long-range transport and local impacts from surrounding measurement sites can occasionally affect nss  $\text{SO}_4^{2-}$  over very short periods, mostly during March–October. However, because its concentration is very low, its effect to concentration variability of nss  $\text{SO}_4^{2-}$  was insignificant. Seasonal variabilities of  $\text{NH}_4^+$  in aerosol were also mainly associated with change of emission strength of  $\text{NH}_3$ , the capacity of acidic components in aerosol to neutralize  $\text{NH}_3$ , and also meteorology.  $\text{NH}_4^+$  in aerosol was a by product of atmospheric reaction of  $\text{NH}_3$  and acid aerosol rather than direct input of suspended ornithogenic soil particles of penguin colony area near KSG. Because  $\text{NH}_3$  can be emitted from the penguin colony area of KGI and biological activity in the ocean surrounding KGI during spring to summer,  $\text{NH}_3$  (g) and  $\text{NH}_4^+$  (p) from these potential emission sources should be measured to evaluate their relative contribution to affect the concentration variabilities of  $\text{NH}_4^+$  in aerosol sampled at KSG.

#### Author contribution

SBH, YJY, Silvia Becagli, Rita Traversi, V. Vitale designed the study. SBH measured mass of  $\text{PM}_{2.5}$  and analyzed ionic species in  $\text{PM}_{2.5}$ . Silvia Becagli, Rita Traversi, Mirko Severi analyzed ionic species in  $\text{PM}_{10}$ . SBH, S.D. Chambers maintained the Rn detector. S.D. Chambers, J. Crawford, A.D. Griffiths analyzed Rn gas. SBH, YTK operated the aerosol sampler at King Sejong Station. SJP maintained Automatic weather station and analyzed meteorological data. KTP, EHJ analyzed distribution of biomass from satellite data. JHK analyzed sea ice concentration from satellite data. SBH wrote the 1st draft of the manuscript.

#### Declaration of competing interest

The authors declare that they have no known competing financial interests or personal relationships that could have appeared to influence the work reported in this paper.

#### Acknowledgements

This research was partly supported by KOPRI research grant (PE19010 and PE19040). We sincerely thank over-wintering staff at King Sejong Station for their support of the installation of aerosol sampler. A special acknowledgement to Prof. Roberto Udisti, now retired, that strongly wanted these measurements, without his efforts such measurements would have not been done. We gratefully acknowledge the Air Resources Laboratory (ARL) for provision of the HYSPLIT transport and dispersion model and mixing height on READY website ([http://ready.arl.noaa.gov/HYSPLIT\\_traj.php](http://ready.arl.noaa.gov/HYSPLIT_traj.php) and <http://ready.arl.noaa.gov/READYamet.php>) used in this publication. Also, we thank the environmental analysis group of the department of Chemistry of Jeju National University for their support of measurement of mass of  $\text{PM}_{2.5}$  and also reanalysis of anions in extracted samples from denuder tubes for their certification. We would also like to thank the reviewers for their insightful and constructive feedback, which has helped improving the clarity and utility of the final manuscript.

#### Appendix A. Supplementary data

Supplementary data to this article can be found online at <https://doi.org/10.1016/j.atmosenv.2019.117185>.

#### References

- Artaxo, P., Rabello, M.L.C., Maenhaut, W., Grieken, R.V., 1992. Trace metals and individual particle analysis of atmospheric aerosols from the Antarctic Peninsula. *Tellus* 44B, 318–334. <https://doi.org/10.1034/j.1600-0889.1992.00010.x>.
- Asmi, E., Neitola, K., Teinila, K., Rodriguez, E., Virkkula, A., Backman, J., Bloss, M., Jokela, J., Lihavainen, H., De Leeuw, G., Paatero, J., Aaltonen, V., Mei, M., Gambarte, G., Copes, G., Albertini, M., Perez Fogwill, G., Ferrara, J., Elena Barlasina, M., Sanchez, R., 2018. Primary sources control the variability of aerosol optical properties in the Antarctic Peninsula. *Tellus* 70B, 1414571. <https://doi.org/10.1080/16000889.2017.1414571>.
- Becagli, S., Scarchilli, C., Traversi, R., Dayan, U., Severi, M., Frosini, D., Vitale, V., Mazzola, M., Lupi, A., Nava, S., Udisti, R., 2011. Study of present-day sources and transport processes affecting oxidised sulphur compounds in atmospheric aerosols at Dome C (Antarctica) from year-round sampling campaigns. *Atmos. Environ.* 52, 98–108. <https://doi.org/10.1016/j.atmosenv.2011.07.053>.
- Carmichael, G.R., Hong, M.-S., Ueda, H., Chen, L.L., Murano, K., Park, J.-K., Lee, H., Kim, Y., Kang, C., Shim, S., 1997. Aerosol composition at cheju island, Korea. *J. Geophys. Res.* 102 (D5), 6047–6061. <https://doi.org/10.1029/96JD02961>.
- Chambers, S.D., Hong, S.-B., Williams, A.G., Crawford, J., Griffiths, A.D., Park, S.-J., 2014. Characterising terrestrial influences on Antarctic air masses using Radon-222 measurements at King George Island. *Atmos. Chem. Phys.* 14, 9903–9916. <https://doi.org/10.5194/acp-14-9903-2014>.
- Chambers, S.D., Preunkert, S., Weller, R., Hong, S.-B., Humphries, R.S., Tositti, L., Angot, H., Legrand, M.L., Williams, A.G., Griffiths, A.D., Crawford, J., Simmons, J., Choi, T.J., Krummel, P.B., Molloy, S., Loh, Z., Galbally, I., Wilson, S., Magand, O., Sprovieri, F., Pirrone, N., Dommergue, A., 2018. Characterizing atmospheric transport pathways to Antarctica and the remote southern ocean using Radon-222. *Front. Earth Sci.* 6 (190) <https://doi.org/10.3389/feart.2018.00190>.
- Choi, M.-Y., 2014. Annual Report of Environmental Monitoring on Human Impacts Around the King Sejong Station, Antarctica. Korea Polar Research Institute, Incheon, pp. 26–27.
- Choi, T.-J., Lee, B.-Y., Kim, S.-J., Yoon, Y.-J., Lee, H.-C., 2008. Net radiation and turbulent energy exchanges over a non-glacial coastal area on King George Island during four summer seasons. *Antarct. Sci.* 20 (1), 99–111. <https://doi.org/10.1017/S095410200700082x>.
- Davis, D., Chen, G., Kasibhatla, P., Jefferson, A., Tanner, D., Eisele, F., Lenschow, D., Neff, W., Berresheim, H., 1998. DMS oxidation in the Antarctic marine boundary layer: comparison of model simulations and field observations of DMS, DMSO, DMSO<sub>2</sub>, H<sub>2</sub>SO<sub>4</sub>(g), MSA(g), and MSA(p). *J. Geophys. Res.* 103 (D1), 1657–1678. <https://doi.org/10.1029/97JD03452>.
- Draxler, R.R., Rolph, G.D., 2003. Hybrid single-particle Lagrangian integrated trajectory (HYSPLIT) Model. <https://www.arl.noaa.gov/ready/hysplit4.html>.
- Hall, J.S., Wolff, E.W., 1998. Causes of seasonal and daily variations in aerosol sea-salt concentrations at a coastal antarctic station. *Atmos. Environ.* 32 (21), 3669–3677. [https://doi.org/10.1016/s1352-2310\(98\)00090-9](https://doi.org/10.1016/s1352-2310(98)00090-9).
- Hong, S.-B., Kim, D.-S., Ryu, S.-Y., Lee, K.-W., Kim, Y.-J., Lee, J.-H., 2009. Design and testing of a semi-continuous measurement system for ionic species in  $\text{PM}_{2.5}$ . Part. Part. Syst. Charact. 25 (5–6), 444–453. <https://doi.org/10.1002/ppsc.200701082>.
- Hong, S.-B., Lee, K.-H., Hur, S.-D., Hong, S., Soyol-Erdene, T.O., Kim, S.-M., Chung, J.-W., Jun, S.-J., Kang, C.-H., 2015. Development of melting system for measurement of trace elements and ions in ice core. *BKCS* 36 (4), 1069–1081. <https://doi.org/10.1002/bkcs.10198>.
- Jang, E., Park, K.-T., Yoon, Y.J., Kim, T.-W., Hong, S.-B., Becagli, S., Traversi, R., Kim, J., Gim, Y., 2019. New particle formation events observed at the King Sejong Station, Antarctic Peninsula – Part 2: Link with the oceanic biological activities. *Atmos. Chem. Phys.* 19, 7595–7608. <https://doi.org/10.5194/acp-19-7595-2019>.
- Jung, J.-Y., Furutani, H., Uematsu, M., Park, J.-S., 2014. Distributions of atmospheric non-sea-salt sulphate and methanesulfonic acid over the Pacific Ocean between  $48^\circ\text{N}$  and  $55^\circ\text{S}$  during summer. *Atmos. Environ.* 99, 374–384. <https://doi.org/10.1016/j.atmosenv.2014.10.009>.
- Kim, J.-S., Yoon, Y.-J., Gim, Y.-T., Kang, J.-H., Choi, J.-H., Park, K.-T., Lee, B.-Y., 2017. Seasonal variations in physical characteristics of aerosol particles at the king Sejong station, antarctic peninsula. *Atmos. Chem. Phys.* 17, 12985–12999. <https://doi.org/10.5194/acp-17-12985-2017>.
- Legrand, M., Ducroz, F., Wagenbach, D., Mulvaney, R., Hall, J., 1998. Ammonium in coastal Antarctic aerosol and snow: Role of polar ocean and penguin emissions. *J. Geophys. Res.* 103 (D9), 11,043–11,056. <https://doi.org/10.1029/97JD01976>.
- Legrand, M., Yang, X., Preunkert, S., Theys, N., 2016. Year-round records of sea salt, gaseous, and particulate inorganic bromine in the atmospheric boundary layer at coastal (Dumont d'Urville) and central (Concordia) East Antarctic sites. *J. Geophys. Res.* 121, 997–1023. <https://doi.org/10.1002/2015JD024066>.
- Legrand, M., Preunkert, S., Weller, R., Zipf, L., Elsasser, C., Merchel, S., Rugel, G., Wagenbach, D., 2017a. Year-round record of bulk and size-segregated aerosol composition in central Antarctica (Concordia site) – Part 2: biogenic sulfur (sulfate and methanesulfonate) aerosol. *Atmos. Chem. Phys.* 17, 14055–14073. <https://doi.org/10.5194/acp-17-14055-2017>.
- Legrand, M., Preunkert, S., Wolff, E., Weller, R., Jourdain, B., Wagenbach, D., 2017b. Year-round records of bulk and size-segregated aerosol composition in central Antarctica (Concordia site) – Part 1: fractionation of sea-salt particles. *Atmos. Chem. Phys.* 17, 14039–14054. <https://doi.org/10.5194/acp-17-14039-2017>.
- Li, F., Ginoux, P., Ramaswamy, V., 2008. Distribution, transport, and deposition of mineral dust in the Southern Ocean and Antarctica: contribution of major sources. *J. Geophys. Res.* 113, D10207. <https://doi.org/10.1029/2007JD009190>.
- Lim, S., Lee, M., Rhee, T.S., 2019. Chemical characteristics of submicron aerosols observed at the King Sejong Station in the northern Antarctic Peninsula from fall to

- spring. *Sci. Total Environ.* 668, 1310–1316. <https://doi.org/10.1016/j.scitotenv.2019.02.099>.
- Marshall, G.J., 2003. Trends in the southern annular mode from observations and reanalyses. *J. Clim.* 16, 4134–4143. [https://doi.org/10.1175/1520-0442\(2003\)016<4134:TITSAM>2.0.CO;2](https://doi.org/10.1175/1520-0442(2003)016<4134:TITSAM>2.0.CO;2).
- Mishra, V.K., Kim, K.-H., Hong, S., Lee, K.-H., 2004. Aerosol composition and its source at the king Sejong station, antarctic peninsula. *Atmos. Environ.* 38, 4069–4084. <https://doi.org/10.1016/j.atmosenv.2004.03.052>.
- Monaghan, E.C., Spiel, D.E., Davidson, K.L., 1986. A model of marine aerosol generation via whitecaps and wave destruction. In: Monahan, E., Niocaill, G.M. (Eds.), *Oceanic Whitecaps*. D. Reidel, Norwell, MA, pp. 167–174.
- Norman, M., Leck, C., 2005. Distribution of marine boundary layer ammonia over the Atlantic and Indian Ocean during the Aerosols99 cruise. *J. Geophys. Res.* 110, D16302. <https://doi.org/10.1029/2005JD005866>.
- Park, K.-T., Lee, K., Yoon, Y.-J., Lee, H.-W., Kim, H.-C., Lee, B.-Y., Hermansen, O., Kim, T.-W., Holmen, K., 2013. Linking atmospheric dimethyl sulfide and the Arctic Ocean spring bloom. *Geophys. Res. Lett.* 40, 155–160. <https://doi.org/10.1029/2012GL054560>.
- Park, K.-T., Lee, K., Kim, T.-W., Yoon, Y.-J., Jang, E.-H., Jang, S., Lee, B.-Y., Hermansen, O., 2018. Atmospheric DMS in the Arctic Ocean and its relation to phytoplankton biomass. *Glob. Biogeochem. Cycles* 32, 351–359. <https://doi.org/10.1002/2017GB005805>.
- Pereira, E.B., Evangelista, H., Pereira, K.C.D., Cavalcanti, I.F.A., Setzer, A.W., 2006. Apportionment of black carbon in the south Shetland Islands, antarctic peninsula. *J. Geophys. Res.* 111, D03303. <https://doi.org/10.1029/2005JD006086>.
- Préndez, M., Wächter, J., Vega, C., Flocchini, R.G., Wakayabashi, P., Morales, J.R., 2009. PM<sub>2.5</sub> aerosols collected in the Antarctic Peninsula with a solar powered sampler during austral summer periods. *Atmos. Environ.* 43, 5575–5578. <https://doi.org/10.1016/j.atmosenv.2009.07.030>.
- Prijith, S.S., Aloysius, M., Mohan, M., 2014. Relationship between wind speed and sea salt aerosol production: a new approach. *J. Atmos. Sol. Terr. Phys.* 108, 34–40. <https://doi.org/10.1016/j.jastp.2013.12.009>.
- Rankin, A.M., Wolff, E.W., Martin, S., 2002. Frost flowers: implications for tropospheric chemistry and ice core interpretation. *J. Geophys. Res.* 107 (D23), 4683. <https://doi.org/10.1029/2002JD002492>.
- Savarino, J., Kaiser, J., Morin, S., Sigman, D.M., Thiemens, M.H., 2007. Nitrogen and oxygen isotopic constraints on the origin of atmospheric nitrate in coastal Antarctica. *Atmos. Chem. Phys.* 7, 1925–1945. <https://doi.org/10.5194/acp-7-1925-2007>.
- Savoie, D.L., Prospero, J.M., Larsen, R.J., Huang, F., Izaguirre, M.A., Huang, T., Snowdon, T.H., Custals, L., Sanderson, C.G., 1993. Nitrogen and sulfur species in antarctic aerosols at Mawson, plamer station, and Marsh (king George island). *J. Atmos. Chem.* 17 (2), 95–122. <https://doi.org/10.1007/BF00702821>.
- Seinfeld, J.H., Pandis, S.N., 1998. *Atmospheric Chemistry and Physics: from Air Pollution to Climate Change*. Wiley-Interscience, New York, p. 444.
- Shaw, G.E., 1988. Antarctic aerosols: a review. *Rev. Geophys.* 26 (1), 89–112. <https://doi.org/10.1029/RG026i001p00089>.
- Sheridan, P., Andrews, E., Schmeisser, L., Vassel, B., Ogren, J., 2016. Aerosol measurements at South Pole: climatology and impact of local contamination. *Aerosol Air Qual. Res.* 16, 855–872. <https://doi.org/10.4209/aaqr.2015.05.0358>.
- Shirsat, S.V., Graf, H.F., 2009. An emission inventory of sulfur from anthropogenic sources in Antarctica. *Atmos. Chem. Phys.* 9, 3397–3408. <https://doi.org/10.5194/acp-9-3397-2009>.
- Song, J.-M., Bu, J.-O., Kim, W.-H., Kang, C.-H., 2016. Influences of long-range transported air pollutants on atmospheric TSP aerosol compositions at Jeju island of Korea during 2011–2013. *BKCS* 37 (5), 626–631. <https://doi.org/10.1002/bkcs.10731>.
- Song, J.-M., Bu, J.-O., Lee, J.-Y., Kim, W.-H., Kang, C.-H., 2017. Ionic compositions of PM<sub>10</sub> and PM<sub>2.5</sub> related to meteorological conditions at the Gosan site, Jeju island from 2013 to 2015. *Asian J. Atmos. Environ.* 11 (4), 313–321. <https://doi.org/10.5572/ajae.2017.11.4.313>.
- Stohl, A., 1998. Computation, accuracy and applications of trajectories - a review and bibliography. *Atmos. Environ.* 32 (6), 947–966. [https://doi.org/10.1016/S1352-2310\(97\)00457-3](https://doi.org/10.1016/S1352-2310(97)00457-3).
- Tang, I.N., 1996. Chemical and size effects of hygroscopic aerosols on light scattering coefficients. *J. Geophys. Res.* 101 (D14), 19245–19250. <https://doi.org/10.1029/96JD03003>.
- Thompson, D.W.J., Solomon, A., 2002. Interpretation of recent southern hemisphere climate change. *Science* 296 (5569), 895–899. <https://doi.org/10.1126/science.1069270>.
- Traversi, R., Udisti, R., Frosini, D., Becagli, S., Ciardin, V., Funke, B., Lanconelli, C., Petkov, B., Scarchilli, C., Severi, M., Vitale, V., 2014. Insights on nitrate sources at Dome C (East Antarctic Plateau) from multi-year aerosol and snow records. *Tellus* 66B, 22550. <https://doi.org/10.3402/tellusb.v66.22550>.
- Traversi, R., Becagli, S., Brogioni, M., Caiazzo, L., Ciardini, V., Giardi, F., Legrand, M., Macelloni, G., Petkov, B., Preunkert, S., Scarchilli, C., Severi, M., Vitale, V., Udisti, R., 2017. Multi-year record of atmospheric and snow surface nitrate in the central Antarctic plateau. *Chemosphere* 172, 341–354. <https://doi.org/10.1016/j.chemosphere.2016.12.143>.
- Udisti, R., Dayan, U., Becagli, S., Busetto, M., Frosini, D., Legrand, M., Lucarelli, F., Preunkert, S., Severi, M., Traversi, R., Vitale, V., 2012. Sea spray aerosol in central Antarctica. Present atmospheric behavior and implications for paleoclimatic reconstructions. *Atmos. Environ.* 52, 109–120. <https://doi.org/10.1016/j.atmosenv.2011.10.018>.
- Vaughan, D.G., Doake, C.S.M., 1996. Recent atmospheric warming and retreat of ice shelves on the Antarctic Peninsula. *Nature* 379, 328–331. <https://doi.org/10.1038/379328a0>.
- Vaughan, D.G., Marshall, G.J., Connolley, W.M., Parkinson, C., Mulvaney, R., Hodgson, D.A., King, J.C., Pudsey, C.J., Turner, J., 2003. Recent rapid regional climate warming on the Antarctic Peninsula. *Clim. Change* 60, 243–274. <https://doi.org/10.1023/A:1026021217991>.
- Vogt, R., Crutzen, P.J., Sander, R., 1996. A mechanism for halogen release from sea-salt aerosol in the remote marine boundary layer. *Nature* 383 (26), 327–330. <https://doi.org/10.1038/383327a0>.
- Wagenbach, D., Ducroz, F., Mulvaney, R., Keck, L., Minikin, A., Legrand, M., Hall, J., Wolff, E., 1998. Sea salt aerosol in coastal Antarctic regions. *J. Geophys. Res.* 103, 10,961–10,974. <https://doi.org/10.1029/97JD01804>.
- Weller, R., Woltjen, J., Piel, C., Resenberg, R., Wagenbach, D., König-Langlo, G., Kriews, M., 2008. Seasonal variability of crustal and marine trace elements in the aerosol at Neumayer station, Antarctica. *Tellus* 60B, 742–752. <https://doi.org/10.1111/j.1600-0889.2008.00372.x>.
- Weller, R., Wagenbach, D., Legrand, M., Elsasser, C., Tian-Kunze, X., König-Langlo, G., 2011. Continuous 25-year aerosol records at coastal Antarctica-I: inter-annual variability of ionic compounds and links to climate indices. *Tellus* 63B, 901–919. <https://doi.org/10.1111/j.1600-0889.2011.00542.x>.
- Wolff, E.W., Legrand, M., Wagenbach, D., 1998. Coastal Antarctic aerosol and snowfall chemistry. *J. Geophys. Res.* 103 (D9), 10927–10934. <https://doi.org/10.1029/97JD03454>.
- Yang, X., Pyle, J.A., Cox, R.A., 2008. Sea salt aerosol production and bromine release: role of snow on sea ice. *Geophys. Res. Lett.* 35, L16815. <https://doi.org/10.1029/2008GL034536>.
- Zhang, M., Chen, L., Xu, G., Lin, Q., Liang, M., 2015. Linking phytoplankton activity in polynas and sulphur aerosols over Zhongshan Station, East Antarctica. *J. Atmos. Sci.* 72, 4629–4642. <https://doi.org/10.1175/JAS-D-15-0094.1>.